Mineral. Soc. Amer. Spec. Pap. **2**, 251–274 (1969).

CHEMOGRAPHIC EXPLORATION OF AMPHIBOLE ASSEMBLAGES FROM CENTRAL MASSACHUSETTS AND SOUTHWESTERN NEW HAMPSHIRE

PETER ROBINSON AND HOWARD W. JAFFE
Department of Geology, University of Massachusetts, Amherst, Massachusetts 01002

ABSTRACT

Fourteen wet chemical and forty electron-probe analyses were made of amphiboles from critical assemblages in the kyanite and sillimanite zones of central Massachusetts and southwestern New Hampshire. The rocks studied include plagioclase amphibolites that are metamorphosed mafic lavas and tuffs, aluminous anthophyllite rocks of uncertain derivation, quartz-garnet-amphibole granulites that are metamorphosed ferruginous cherts, and pods of ultramafic amphibolite. The rocks contain the following associations: hornblende-anthophyllite, hornblende-cummingtonite, anthophyllite-cummingtonite, hornblende-anthophyllite-cummingtonite, anthophyllite-cordierite, and anthophyllite-kyanite-sillimanite-staurolite-garnet.

The following generalizations are made: 1) The cummingtonites are compositionally simple, containing neither significant Al/Al, Na/Al, nor Ca substitution. 2) The hornblendes are high in Al/Al substitution. Those coexisting with cummingtonite in the kyanite zone or in retrograded rocks have a higher Al content than those coexisting with cummingtonite in the sillimanite zone, in close agreement with the prograde reaction tschermakitic hornblende $\rightarrow$ cummingtonite + plagioclase + H_2O proposed by Shido. The Na content of hornblende is considerably less than that of the theoretical edenite end member and is relatively insensitive to variation in the Na content of coexisting plagioclase. 3) Anthophyllites coexisting with hornblende contain about $\frac{2}{3}$ as much Al/Al substitution and $\frac{1}{2}$ as much Na substitution as coexisting hornblendes. Ca is negligible. Anthophyllites with cordierite, aluminosilicates, or garnet equal or surpass hornblende in Al/Al and Na substitution. Anthophyllites coexisting with cummingtonite are more aluminous than the cummingtonite, and anthophyllites as a group can be distinguished from cummingtonites by their higher Na content and Na/Ca ratios. 4) Chemographic data for the sillimanite zone indicate there should be a narrow three-amphibole field centered on 100 Fe/(Fe + Mg) = 41 with hornblende and anthophyllite in more magnesian assemblages, and either hornblende and cummingtonite or cummingtonite and anthophyllite in more iron-rich assemblages. A true three-amphibole assemblage was located some miles away in the sillimanite-orthoclase zone with the three phase field centered on 100 Fe/(Fe + Mg) = 36.

The wet analyses show that one fifth to nearly one half of the Fe in hornblende is Fe^{3+}, anthophyllite has much less Fe^{3+}, and cummingtonite still less.

Metamorphic rock compositions more or less restricted to the system $SiO_2 - Ai_2O_3 - FeO - MgO$, such as the aluminous anthophyllite rocks reported here, are rare, but sufficiently known worldwide to allow recognition of several facies for quartz-saturated rocks, all containing combinations of anthophyllite, cummingtonite, cordierite, Al-silicates, staurolite, and garnet.

INTRODUCTION

The purpose of this study was to determine the composition and extent of solid solution of coexisting amphiboles and associated minerals from a variety of rocks, all of which were subjected to approximately the same metamorphic conditions. Such a study was done on rocks of pelitic composition for the kyanite zone in Vermont by Albee (1965a). Klein (1968) recently completed a survey of coexisting amphiboles on a worldwide basis that formed under a variety of conditions.

The amphibole rocks of this study were found during detailed mapping of the Orange area, central Massachusetts and southwestern New Hampshire (Robinson, 1963, 1967) and adjacent areas. The Orange area (Fig. 1) lies on the Bronson Hill anticlinorium, a zone of en echelon gneiss domes with cores composed of gneiss of uncertain age mantled by metamorphosed sedimentary and volcanic rocks of Middle Ordovician, Silurian, and Early Devonian age (Thompson, Robinson, Clifford, and Trask, 1968). The Triassic border fault with a probable displacement of 5 to 8 km (east side upthrown) lies in the northwest corner of the area.

The western part of the Orange area was metamorphosed in the kyanite zone, but kyanite is relatively scarce because of bulk composition and common mica schists contain abundant staurolite. The eastern part of the area was metamorphosed in the sillimanite zone, the kyanite-sillimanite boundary being defined by the westernmost occurrences of fibrolitic sillimanite. Sillimanite is abundant and commonly occurs in mica schists with muscovite, biotite, staurolite, and garnet. Within the sillimanite zone there are scattered occurrences of kyanite, some coexisting with sillimanite, that are considered to be relics of earlier stages of metamorphism that survived later higher temperature conditions. In the eastern part of the area there are a few rocks that contain coexisting quartz, muscovite, sillimanite, orthoclase and oligoclase suggesting a transition toward the sillimanite-orthoclase zone. In the extreme south central part of the area there was thorough retrograde metamorphism of sillimanite zone rocks to mineralogy characteristic of the biotite zone.

The structural history of the area is complex. Earlier nappe structures with amplitudes up to 25 km are deformed about later gneiss domes that may be bulging or strongly overturned with vertical amplitudes up to 10–12 km. The nappe and dome structures involve Lower Devonian rocks and both formed during the metamorphism that was probably Middle Devonian. Conditions of metamorphism are estimated to have been 600–700°C and 5–7 kbar total pressure (Robinson, 1966).

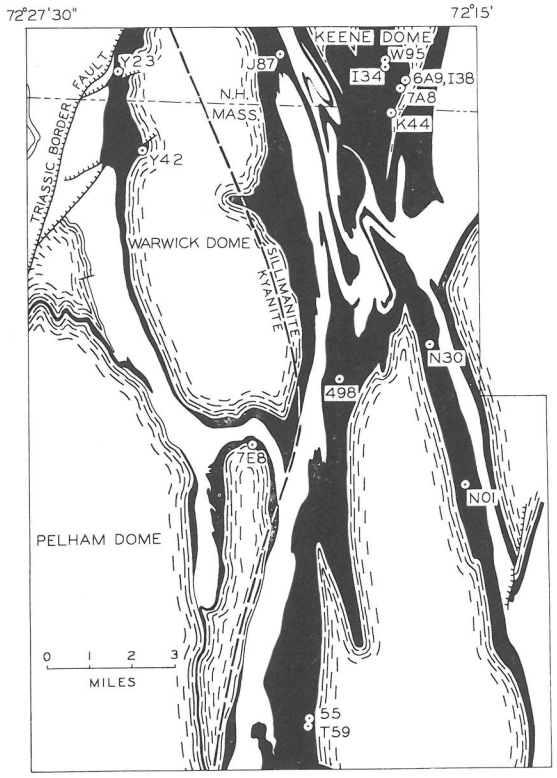

FIG. 1. Generalized geologic map of the Orange area, Massachusetts and New Hampshire, showing specimen locations and distribution of Middle Ordovician Ammonoosuc Volcanics and Partridge Formation (undifferentiated, black areas). Heavy dashed line is estimated position of the kyanite-sillimanite boundary.

The amphibole rocks of interest occur in several geologic associations. Most important are metamorphosed mafic volcanic layers, either lavas or tuffs, in the Middle Ordovician Ammonoosuc Volcanics or the Partridge Formation. These are plagioclase amphibolites with various combinations of hornblende, cummingtonite, and anthophyllite accompanied in many cases by quartz, biotite, garnet, rutile, ilmenite, or magnetite. Hornblende amphibolites not specifically studied here may also contain epidote, diopside, or sphene. Interbedded with the volcanics at a few localities are peculiar alumina-rich anthophyllite gneisses containing cordierite, kyanite, sillimanite, staurolite, biotite, corundum, and garnet in various combinations. These are believed to represent volcanic materials that were chemically altered, probably in the primary environment. The detailed petrography of the anthophyllite-cordierite gneisses is given elsewhere (Robinson and Jaffe, 1969). Commonly associated with the Middle Ordovician volcanics are ferruginous or manganiferous sedimentary layers, possibly metamorphosed cherts, composed primarily of quartz and garnet, with some cummingtonite, anthophyllite, or hornblende as well as magnetite, apatite, ilmenite, or biotite. Ferruginous layers also occur in the Loer Devonian Littleton Formation, and at one locality such a layer contains an association of olivine (Fe_{88}, no quartz), orthopyroxene (Fe_{86}), grunerite (Fe_{84}), garnet and magnetite, to be reported in detail elsewhere. The final amphibole association is in pods of ultramafic rocks, probably metamorphosed pyroxenites that appear to intrude most pre-Silurian units in the stratigraphy.

A high proportion of the specimens considered here were collected on two hills less than 3,000 feet (0.9 km) apart in Richmond, New Hampshire and at a third outcrop 6,000 feet (1.8 km) to the south near the state line (Fig. 1). These three localities collectively are referred to as the "Amphibole Hill Area."

PETROGRAPHY

Estimated modes, and other notes on the analyzed specimens are given in Table 1. Plagioclase compositions were determined by measurement of the α refractive index in oils and are expressed in mole percent An. The optical properties of the amphiboles have been studied by the authors but will be reported elsewhere (see also Jaffe, Robinson, and Klein, 1968; Robinson and Jaffe, 1969). All are coarsely crystalline and nearly free of secondary alteration products. Textures vary considerably. Two amphiboles are considered to constitute an assemblage only if they are in mutual contact. Specimen I38A, for example, contains three amphiboles in different layers. A cummingtonite-bearing layer 2 cm thick is in contact with anthophyllite on one side (Klein, 1968, Fig. 14) and hornblende (Ross, Papike, and Weiblen, 1968) on the other. Thus, there are *two* two-amphibole assemblages. One specimen, QB27C, does contain three truly coexisting amphiboles (Robinson, Jaffe, Klein, and Ross, 1969).

Hornblende coexisting with cummingtonite or anthophyllite contains thin exsolution lamellae of colorless clinoamphibole, optically like cummingtonite, oriented parallel to $(\bar{1}01)$ and (100) of the host (Ross, Papike and Weiblen, 1968; Jaffe, Robinson, and Klein, 1968). The intensity of color is variable and strongly dependent on composition but the tone generally follows the pleochroic scheme *Z*–bluish green, *Y*–olive green, *X*–tan. Slight color zoning occurs in some specimens and some grains are twinned on (100).

Cummingtonite coexisting with hornblende contains thin exsolution lamellae of hornblende oriented parallel to $(\bar{1}01)$ and (100) of the host. In many cases hornblende and cummingtonite hosts are in contact along these exsolution planes. Some grains are twinned 1–3 times on (100). Both $(\bar{1}01)$ and (100) exsolution lamellae were observed either in thin section or in oils in all specimens containing both cummingtonite and hornblende hosts. However, because of the variable abundance and distribution of lamellae, some of the grains used for X-ray single crystal work by Ross (see below) are free of lamellae or contain only one set. Cummingtonite coexisting with anthophyllite appears optically to be free of lamellae and is usually polysynthetically twinned on a fine scale (Klein, 1968, Fig. 14). Cummingtonite alone is virtually colorless, but with hornblende lamellae, often not easily detected in thin section, has a green pleochroic scheme.

Anthophyllite coexisting with either cummingtonite or hornblende is free of obvious lamellae. It is colorless to weakly colored and pleochroic with *Z* pinkish tan to pale gray, *Y* tan, and *X* colorless. Magnesian aluminous anthophyllites with cordierite have a similar pleochroic scheme but more iron-rich aluminous anthophyllites have *Z* medium gray, *Y* greenish gray, and *X* tan.

Rabbit (1948) recommended that the term gedrite, for aluminous anthophyllite, be dropped. Because aluminous and non-aluminous anthophyllites are not readily distinguished by optical properties, we have found it practical to use the general term anthophyllite in routine petrographic work and also to describe the chemically continuous anthophyllite phase region. In this paper the term gedrite is applied only to those individual specimens known to be high chemically in Al_2O_3 or to homogeneous crystals or exsolution lamellae known to have a small *b* crystallographic dimension characteristic of the gedrite structure.

Single-Crystal X-Ray Data

A number of amphiboles from the analyzed specimens have been studied in X-ray single-crystal photographs by Malcolm Ross of the U. S. Geological Survey (Ross, Papike, and Weiblen, 1968; Jaffe, Robinson, and Klein, 1968; Robinson and Jaffe, 1969; Robinson, Jaffe, Klein, and Ross, 1969; Ross, Papike, and Shaw, 1969, Table 6, this volume). The general results of these studies are summarized below and notes on individual specimens are included in Table 1.

All of the hornblendes studied belong to space group *C2/m*. The hornblendes associated with cummingtonite contain exsolution lamellae of cummingtonite, space group *C2/m*, oriented parallel to $(\bar{1}01)$ and (100) of the host. The hornblendes associated with anthophyllite contain exsolution lamellae of primitive cummingtonite, space group *P2/m*, oriented parallel to $(\bar{1}01)$ and (100) of the host. The X-ray reflections violating *C2/m* symmetry are relatively sharp, although quite weak, perhaps suggesting a partial inversion to the *C2/m* structure type (Ross, Papike, and Shaw, 1969).

With the exception of specimen QB27C, all of the cummingtonite hosts studied belong to space group *C2/m*. Where cummingtonite coexists with hornblende it contains exsolution lamellae of hornblende, space group *C2/m*, oriented parallel to $(\bar{1}01)$ and (100) of the host.

All of the orthorhombic amphiboles studied belong to space group *Pmna*. Surprisingly, all but the two most aluminous (I34JX, I34I) show fine splitting of reflections indicating they consist of an intergrowth of anthophyllite with a larger, and gedrite with a smaller *b* crystallographic dimension. The only optical indications of this apparent unmixing are extremely fine streaks parallel to (010) in specimens W95JX and I38DX that are barely resolved in end sections using a 50 power objective. Relative intensities of the two sets of X-ray peaks allow estimates of relative abundances of the two phases. Two aluminous orthoamphiboles (W95JX, I38DX) consist of 80 percent gedrite and 20 percent anthophyllite. Anthophyllites coexisting with hornblende (N30X, 6A9X) or cummingtonite (I38A) contain 50–70 percent anthophyllite and 50–30 percent gedrite.

Specimen QB27C contains three coexisting amphiboles. The cummingtonite has weak and diffuse primitive reflections suggesting partial inversion to a *C*-centered structural state. It also has exsolution lamellae of hornblende *C2/m*, parallel to (101) and (100) of the host although the grain studied by Ross contains only (100) lamellae. The hornblende host with *C2/m* symmetry has exsolution lamellae of primitive cummingtonite with diffuse reflections violating *C2/m* symmetry. In addition, the anthophyllite shows a splitting of reflections indicating it consists of approximately 80 percent anthophyllite and 20 percent gedrite.

Chemical Analyses

Chemical analyses were performed by two different methods, wet chemical analyses of purified separates (Table 2, Table 3[1]) and electron-probe analyses of spot locations on polished thin sections (Table 4, Table 5[1]). Electron-probe analyses were made first and most have already been reported by Klein (1968). The reader is referred to his paper for details of the analytical procedure and standards. The electron-probe analyses were partial analyses for Si, Al, Fe, Mn, Mg, Ca, and Na only, whereas the wet analyses were unusually complete.

In many cases specimens for wet chemical analyses were collected within inches of the original sample described by Robinson (1963) on which the electron-probe analyses were done. Such large, carefully cleaned, hand specimens are indicated by the letter X following the specimen number. Electron-probe and wet chemical analyses from the same locality compare quite well, but differences between them could be due to differences in the material analyzed. In addition, however, there are inherent differences in the two analytical procedures that should give different results. The wet chemical analyses should show the maximum amount of impurity, whether exsolution lamellae of another amphibole or fragments of foreign minerals. The wet chemical analyses are thus useful for showing the minimum width of amphibole miscibility gaps under conditions in which coarse crystallization took place. In some cases the probe analyses are surprisingly close to the wet analyses even in cases where exsolution lamellae are very abundant (in particular cummingtonite 7A8B and 7A8BX). This suggests that even though an attempt was made to analyze homogeneous amphibole the area analyzed was sufficiently large that it was impossible to avoid a large proportion of lamellae. Thus, the probe analyses give only an indication of the minimum possible width of the miscibility gap following exsolution. Comparison of wet and probe analyses of specmens from the same locality (Figs. 4F, 6F) suggests analytical uncertainty is greater than compositional differences that might be expected and indicates that the amount of coarse exsolution is slight.

The probe analyses show total Fe as FeO. The wet analyses show both FeO and Fe_2O_3. For direct comparison with probe analyses it is necessary to recalculate the total Fe in wet analyses as FeO. Once this "ferric correction" is determined it is possible either numerically or graphically to make an estimate of ferric iron in the probe specimens and correct them to show "true FeO." Some of the phase diagrams make little sense topologically without this ferric correction.

Mineral separation and purification for wet analysis. All specimens were examined in the field and later in thin-section or oils to ensure that only those essentially free of secondary or retrograde alteration minerals were selected for separations. All of the mineral separations were made on the basis of differences in density and paramagnetic susceptibility of the constituents. Because in many instances these differences are slight, heavy liquid and magnetic separations had to be repeated many times. In one instance the final concentrate of hornblende coexisting with cummingtonite had to be purified by handpicking. The purity of each mineral concentrate was established by counting 1000 grains of each separate under the petrographic microscope (Chayes, 1944).

Paramagnetic susceptibility of the amphiboles on the Frantz magnetic separator was found to vary essentially linearly with the total percentage of $Fe^{3+} + Mn^{2+} + Fe^{2+} + Ni^{2+} + Cr^{3+}$.

[1] Tables 3 and 5 give the various component ratios (obtained from Tables 2 and 4, respectively) which are used to plot the chemographic relations depicted in Figures 2–13. Tables 3 and 5 may be ordered as NAPS Document 00461 from ASIS National Auxiliary Publications Service, c/o CCM Information Sciences, Inc., 22 West 34th Street, New York, N.Y. 10001, remitting in advance $1.00 for microfiche or $3.00 for photocopies, payable to ASIS-NAPS.

TABLE 1. ESTIMATED MODES OF SPECIMENS CONTAINING ANALYZED AMPHIBOLES

	W95JX	E	I34JX	I34I	I38DX	N30X	6A9X	7E8BX	7A8BX	Y42BX
Anthophyllite	70 p	96 p	25 p	33 g	28 g		20 p			
Cummingtonite						See N30B and N30C		See 7E8B	3 pgg	See Y42B
Hornblende							39 bg		39 dg	
Quartz			27	50	61				8	
Plagioclase (An %, range) (An %, ave.)			8 (27–31)				40 (35) (35)		47 (22) (22)	
Garnet				4	10					
Biotite			X	8			1		X	
Chlorite					tr		X			
Talc										
Rutile	3	1	X							
Ilmenite			X	1	X		X		X	
Magnetite	tr		X						3	
Zircon	X		X							
Monazite					tr		tr			
Allanite										
Apatite	X		X	X	X		X		X	
Tourmaline	tr		tr							
Calcite										
Cordierite	27	3	40							
Kyanite	X		X	X						
Sillimanite	X		X	1						
Staurolite	X		X	3						
Corundum	X		tr							
Spinel	X									

X—common but in amount less than 1%, tr—present as trace only, not common.
Abbreviations for strongest color in amphiboles: g gray, pg pale gray, vpg very pale gray, bg blue green, pbg pale blue green, dg dark green, p pinkish tan, pp pale pinkish tan, cl colorless, pgg pale greenish gray, pbb pale brown to bluish green.

Description of Specimens in Table 1.

All specimens from Ammonnosuc Volcanics unless otherwise noted. Referred to in Robinson (1963) unless different reference is indicated.

W95JX—Coarse-grained bedded anthophyllite-cordierite gneiss with aluminous enclaves in cordierite (Robinson and Jaffe, 1969). Orthorhombic amphibole, space group *Pnma*, consists of gedrite host, 80%, and anthophyllite lamellae, 20%. Lamellae ‖ to (010) visible under high magnification.

E—Analysis of separate from "gedrite-rutile rock" collected by Emerson (1895). Mode is of specimen I34E of Robinson (1963) believed to be representative of material collected by Emerson. Dark brown, fine-grained, weakly foliated anthophyllite rock. 3% "cordierite" is actually an unidentified alteration product probably after cordierite.

I34JX—Coarse-grained cordierite-anthophyllite-quartz-andesine gneiss with aluminous enclaves in cordierite (Robinson and Jaffe, 1969). Orthorhombic amphibole consists of >99% gedrite, space group *Pnma*, with exsolved rutile needles. Wet chemical analysis of coexisting cordierite: $(Na,K)_{0.13}(Mg_{1.51},Fe_{0.30}^{2+},Fe_{0.04}^{3+},Li_{0.03},Ca_{0.02})Al_{4.00}Si_{5.01}O_{18}\cdot 0.83\ H_2O$. Biotite, $\gamma=1.610$.

I34I—Black, medium-grained, well foliated quartz-anthophyllite-biotite-garnet-staurolite-sillimanite schist. Orthorhombic amphibole is 100% gedrite, space group *Pnma*. Garnet, $n=1.793$ (zoned ~1.791 —1.795), $a=11.515$ Å, visual arc spectrographic analysis: Fe, Mg >5%, Mn 1–5%, Ca 0.1–1%, Na and Li <1%. Estimated composition: $Alm_{58}Pyr_{27}Spess_{14}Gross_1$. Biotite, $\gamma=1.621$.

I38DX—Well bedded, coarse-grained quartz-garnet-anthophyllite granulite with irregular garnets up to 3 mm diam. enclosed in gray anthophyllite. Orthorhombic amphibole, space group *Pnma*, consists of gedrite host, 80%, and anthophyllite lamellae, 20%. Lamellae ‖ to (010) visible under high magnification.

N30X—Partridge Formation, medium-grained hornblende-anthophyllite amphibolite. Hornblende host, space group $C2/m$, 90%; primitive cummingtonite lamellae on $(\bar{1}01)$, space group $P2_1/m$, 5%; primitive cummingtonite lamellae on (100), $P2_1/m$, 5%. (100) and $(\bar{1}01)$ lamellae are 0.25 —0.4μ and 0.4–0.8μ thick, respectively. Anthophyllite host, space group *Pnma*, 50%; submicroscopic gedrite exsolution, *Pnma*, 50%.

6A9X—Medium-grained hornblende-anthophyllite amphibolite. Hornblende host, space group $C2/m$, 90%; primitive cummingtonite lamellae on (100), space group $P2_1/m$, 7%; primitive cummingtonite on $(\bar{1}01)$, $P2_1/m$, 3%. (100) and $(\bar{1}01)$ lamellae are 0.4 and 0.8μ thick respectively. Anthophyllite host, 70%; submicroscopic gedrite exsolution, 30%, both *Pnma*.

7E8BX—Coarse-grained layered plagioclase-cummingtonite-hornblende-biotite-garnet gneiss. Hornblende host, 99%; cummingtonite lamellae on (100), 1%; both $C2/m$. Cummingtonite host, $C2/m$,

FROM CENTRAL MASSACHUSETTS AND SOUTHWESTERN NEW HAMPSHIRE

N30C	N30B	N01A	I34B	J87D	QB27C	155	T59B	6A9	K44C	K44E	498	Y23C	7E8B	Q795	7A8B	Y42B	I38A	
40 p	15 p		22 p	40 pg	25 p	7 vpg	5 vpg	20 pp	18 p							4 vpg	3 cl	
		2 cl			13 cl					5 cl	3 cl	27 cl	10 pgg	13 cl	20 pgg	6 cl	4 cl	5 cl
35 bg	45 bg	75 pbb	40 pbg	2 bg	12 pbg	23 bg	37 bg	40 bg	22 bg	1 bg	50 pbb	5 bg	7 bg	5 bg	25 dg	tr		2 pbg
				12		5	3		20	33	8	45	15	10	8	39	85	85
25 (44–53)	38 (38–51) (47)		38 (44–59) (53)	40 (37–42)	46 (73–80) (75)	58 (33–39) (33)	50 (37–43) (40)	37 (35) (35)	39 (27–37) (34)	60 (32) (32)	36 (78) (78)	tr (22) (22)	46 (25) (25)	20 (29-43) (34)	44 (22) (22)	50 (16) (16)		
												13	2	45			7	7
2	tr			5	3	X		2	X		1		5	X	tr			
		20						X					X	X		tr		
		3																
X	2		X	X				tr										
		tr			1			X	1	X	2	tr	1			X		
						7	5					10		7	3		1	1
																tr		
										tr								
X	X	X		X	X		X	tr	X	X	X	X	X	X	X	X	X	X
				X														
															tr			
				tr?														

100%. In thin section and oils both hosts contain lamellae. (100) lamellae are about 0.25μ thick, ($\bar{1}$01) lamellae are about 0.35μ thick. Biotite, $\gamma = 1.630$.

7A8BX—Medium-grained hornblende-cummingtonite amphibolite zone in outer part of metamorphosed lava pillow. Pillow core is hornblende amphibolite, matrix surrounding pillows is hornblende, garnet, and biotite. Hornblende host, 90–94%; cummingtonite lamellae on ($\bar{1}$01), 3–10%, cummingtonite lamellae on (100), 0–3%, all space group $C2/m$. Cummingtonite host, 88–92%; hornblende lamellae on (100), 2–4%; hornblende lamellae on ($\bar{1}$01), 4–10%; all $C2/m$. (100) and ($\bar{1}$01) lamellae are 0.4–0.6 μ and 0.8–2.0 μ thick respectively.

Y42BX—Identical to Y42B except that no anthophyllite could be detected either in oils or by X-ray tests on concentrate. Cummingtonite is identical optically to cummingtonite that co-exists with anthophyllite in Y42B. No exsolution lamellae were observed.

N30C, N30B—See N30X

N01A—Ten-foot ultramafic layer in amphibolite and schist of Partridge Formation. Dark green, fine-grained, weakly layered well foliated hornblende-chlorite-talc schist with light brown circular talc-rich patches. Hornblende contains extremely thin (100) lamellae and very rare ($\bar{1}$01) lamellae. No lamellae were resolved in cummingtonite. Hornblende has peculiar pale brown and blue-green color.

I34B—Medium-grained, weakly layered and foliated hornblende-plagioclase-anthophyllite gneiss. Hornblende contains (100) lamellae 0.25 μ thick and ($\bar{1}$01) lamellae 0.4 μ thick.

J87D—Coarse-grained anthophyllite-biotite-hornblende gneiss. No exsolution lamellae were observed in hornblende.

QB27C—Volcanic zone in Partridge Formation, sillimanite-orthoclase zone, east shore of Quabbin reservoir, approximately one mile south of intake works, Winsor Dam quadrangle, Mass. Medium-grained three amphibole amphibolite at contact between hornblende-cummingtonite amphibolite and quartz-anthophyllite-andesine gneiss (Robinson, Jaffe, Klein, and Ross, 1969). Two analysis sets. Hornblende host, space group $C2/m$, 75%; primitive cummingtonite lamellae on (100), $P2_1/m$, 25%. Primitive cummingtonite host, space group $P2_1/m$, 85%; hornblende lamellae on (100), space group $C2/m$, 15%. Anthophyllite host, 80%; submicroscopic gedrite exsolution, 20%, both $Pnma$.

155—Medium-grained hornblende-magnetite amphibolite with plagioclase-rimmed anthophyllite needles up to 8 cm long. Slightly weathered. Hornblende contains (100) and ($\bar{1}$01) exsolution lamellae 0.4 μ and 0.6 μ thick respectively. Hornblende has a strong blue tint.

T59B—Same as 155. Fresh.

6A9—See 6A9X

K44C—Medium-grained hornblende-anthophyllite amphibolite. Hornblende contains (100) and ($\bar{1}$01) exsolution lamellae 0.4 μ and 0.6–1.0 μ thick respectively.

K44E—Contact zone between medium-grained plagioclase-quartz-

(*Continued on page 257*)

TABLE 2. WET CHEMICAL ANALYSES AND IONIC RATIOS OF AMPHIBOLES

	Gedrite				
	W95JX[a]	E[b]	I34JX[a]	I34I[a]	I38DX[c]
SiO_2	47.68	47.86	44.72	40.75	45.14
TiO_2	.24	.63	.46	.25	.30
Al_2O_3	13.36	14.09	15.46	19.81	14.28
Fe_2O_3	1.60	.33	2.41	1.22	1.29
Cr_2O_3	.02	—	.002	.011	.007
FeO	12.07	13.41	15.87	19.29	20.19
MnO	.22	.14	.37	.25	.34
MgO	20.68	19.89	16.69	13.81	14.54
NiO	.01	—	.003	.001	.005
CaO	.55	.57	.47	.27	.34
SrO	.001	—	.001	.001	—
BaO	.001	—	.001	.001	—
Li_2O	.01	—	.04	.03	.06
Na_2O	1.24	.93	1.47	1.92	1.45
K_2O	.00	.06	.01	.04	.02
H_2O (+)	2.12	2.46	2.11	2.68	2.47
H_2O (−)	—	—	—	—	.30
P_2O_5	.02	.05	.07	.04	.05
F	.04	—	.09	.01	.02
Cl	.01	—	.01	.01	—
	99.85	100.42	100.24	100.38	100.81
−O=F, Cl	.02	—	.04	.00	.01
Total	99.83	100.42	100.20	100.38	100.80

	Ions per 24 O(OH)				
	W95JX	E	I34JX	I34I	I38DX
Si	6.683	6.647	6.389	5.874	6.480
P	.002	.006	.009	.005	.007
Al	1.315	1.347	1.602	2.121	1.513
Al	.892	.960	1.001	1.245	.904
Cr^{3+}	.002	.000	.000	.002	—
Fe^{3+}	.168	.035	.259	.132	.140
Mg	4.320	4.117	3.553	2.967	3.110
Li	.005	—	.022	.017	.035
Ti^{4+}	.025	.066	.050	.027	.033
Ni	.001	—	.000	.000	.001
Fe^{2+}	1.415	1.557	1.896	2.326	2.424
Mn^{2+}	.026	.017	.045	.030	.041
Ca	.083	.085	.071	.042	.053
Na	.337	.250	.406	.537	.404
K	.000	.010	.001	.007	.003
(OH)	1.982	2.278	2.011	2.578	2.365
F	.018	—	.040	.005	.009
fe[d]	25.01	27.66	35.33	44.26	44.21
fe[e]	27.14	28.10	38.24	45.68	45.58
an[f]	19.68	25.37	14.90	7.19	11.53

	Anthophyllite		*Cummingtonite*		
	N30X[a]	6A9X[c]	7E8BX[a]	7A8BX[c]	Y42BX[c]
SiO_2	51.00	51.12	53.02	52.09	53.54
TiO_2	.20	.23	.08	.18	.10
Al_2O_3	7.99	6.79	2.53	2.62	2.20
Fe_2O_3	.93	1.18	.91	1.50	1.12
Cr_2O_3	.057	.018	.001	.001	.001
FeO	14.94	17.82	24.40	26.02	23.12
MnO	.36	.75	.30	.53	.41
MgO	21.17	18.54	15.50	13.52	16.77
NiO	.049	.015	.004	.004	.003
CaO	.75	.73	.83	1.32	.52
SrO	.001	—	.001	—	—
BaO	.001	—	.001	—	—
Li_2O	.01	.02	.07	.01	.03
Na_2O	.68	.78	.28	.26	.23
K_2O	.00	.02	.00	.04	.02
H_2O (+)	2.46	2.41	2.21	2.41	2.46
H_2O (−)	—	.38	—	.30	.28
P_2O_5	.01	.01	.01	.01	.01
F	.01	.03	.09	.01	.01
Cl	.01	—	.01	—	—
	100.62	100.85	100.23	100.80	100.81
−O=F, Cl	.00	.01	.04	.00	.00
Total	100.62	100.84	100.19	100.80	100.81

	Anthophyllite		*Cummingtonite*		
	N30X	6A9X	7E8BX	7A8BX	Y42BX
Si	7.130	7.267	7.746	7.676	7.733
P	.002	.002	.002	.002	.002
Al	.868	.731	.252	.322	.265
Al	.449	.407	.183	.133	.110
Cr^{3+}	.007	.002	—	—	—
Fe^{3+}	.097	.126	.100	.166	.122
Mg	4.411	3.928	3.375	2.969	3.610
Li	.005	.012	.040	—	.017
Ti^{4+}	.021	.025	.009	.020	.011
Ni	.005	.002	—	—	—
Fe^{2+}	1.747	2.118	2.982	3.206	2.793
Mn^{2+}	.043	.091	.037	.006	.050
Ca	.113	.111	.130	.208	.081
Na	.185	.215	.079	.074	.065
K	—	.003	—	.007	.003
(OH)	2.294	2.286	2.154	2.368	2.369
F	—	.001	.041	—	—
fe[d]	28.83	36.00	47.90	52.43	44.06
fe[e]	29.96	37.29	48.03	53.67	45.22
an[f]	37.86	34.03	62.18	73.67	55.69

	Hornblende			
	N30X[a]	6A9X[a]	7E8BX[c]	7A8BX[c]
SiO_2	44.75	44.78	42.53	44.64
TiO_2	.72	.83	.32	.97
Al_2O_3	13.67	13.33	14.56	9.95
Fe_2O_3	3.86	3.32	4.28	4.94
Cr_2O_3	.111	.036	.001	.003
FeO	7.71	10.67	14.99	17.25
MnO	.16	.31	.14	.23
MgO	14.24	12.53	8.83	8.57
NiO	.043	.01	.001	.003
CaO	10.60	9.81	9.57	9.45
SrO	.004	—	—	—
BaO	.001	—	—	—
Li_2O	.01	.01	.10	.01
Na_2O	1.48	1.80	2.05	1.54
K_2O	.11	.19	.21	.31
H_2O (+)	2.40	2.57	2.65	2.30
H_2O (−)	—	.32	.36	.37
P_2O_5	.01	.03	.03	.01
F	.01	.01	.06	.01
Cl	.01	—	—	—
	99.86	100.54	100.68	100.53
−O=F, Cl	.00	.00	.03	.00
Total	99.86	100.54	100.65	100.53

	Hornblende			
	N30X	6A9X	7E8BX	7A8BX
Si	6.393	6.434	6.243	6.662
P	.002	.003	.004	.004
Al	1.605	1.563	1.753	1.334
Al	.698	.694	.766	.417
Cr^{3+}	.012	.002	—	—
Fe^{3+}	.416	.359	.473	.554
Mg	3.032	2.682	1.932	1.906
Li	—	—	.058	—
Ti^{4+}	.077	.090	.035	.109
Ni	.005	.001	—	—
Fe^{2+}	.921	1.282	1.840	2.153
Mn^{2+}	.019	.038	.018	.028
Ca	1.623	1.510	1.505	1.511
Na	.410	.501	.584	.447
K	.021	.035	.039	.059
(OH)	2.287	2.464	2.595	2.291
F	—	—	.028	—
fe[d]	23.63	32.97	49.02	53.38
fe[e]	30.89	38.49	54.68	58.95
an[f]	79.81	75.09	72.04	77.19

[a] H. Asari, analyst, 1967.
[b] E. A. Schneider, analyst, 1892.
[c] M. Kumanomido, analyst, 1968.

[d] fe=100 (FeO+MnO)/(FeO+MnO+MgO).
[e] Same as above but with total Fe as FeO.
[f] an=(100) Ca/(Na+Ca).

TABLE 4. ELECTRON PROBE ANALYSES[a]

		N30C	N30B	N01A	I34B	J87D	QB27C 2B	QB27C 2A	155	T59B	6A9	K44C	K44E	498	Y23C	7E8B	Q795	7A8B	Y42B	I38A
Anthophyllite	SiO_2	49.1	51.2		48.8	49.5	52.5	52.1	50.8	49.0	49.9	48.4							50.8	51.4
	Al_2O_3	9.3	6.8		10.4	9.3	5.6	5.5	5.9	8.4	7.0	8.8							3.8	3.9
	FeO	14.9	16.3		16.4	17.9	18.8	18.6	19.7	19.5	20.6	21.1							26.3	26.3
	MnO	0.4	0.4		0.5	0.3	0.5	0.5	0.9	1.2	0.7	0.6							0.5	0.6
	MgO	19.8	20.0		18.8	18.8	19.2	18.7	18.2	17.4	17.5	17.6							15.3	14.9
	CaO	0.6	0.4		0.6	0.2	0.4	0.4	0.3	0.7	0.6	0.5							0.0	0.0
	Na_2O	1.0	0.6		1.2	0.7	0.4	0.5	0.4	0.8	0.9	1.1							0.4	0.3
	Total	95.1	95.7		96.7	96.7	97.4	96.3	96.2	97.0	97.2	98.1							97.1	97.4
Cummingtonite	SiO_2			56.2			54.4	54.4					54.9	54.1	54.3	53.5	52.5	52.3	52.1	52.2
	Al_2O_3			0.6			2.7	3.0					1.4	1.1	1.0	1.6	0.8	2.1	1.5	1.0
	FeO			17.4			18.9	18.5					22.4	22.5	22.9	25.5	26.8	25.1	25.0	26.8
	MnO			0.7			0.5	0.5					0.8	0.9	2.3	0.6	0.3	0.6	0.6	0.6
	MgO			21.2			19.2	19.1					18.3	18.2	17.4	16.5	16.3	14.9	15.7	15.2
	CaO			0.8			1.4	1.4					1.0	0.7	0.4	0.3	0.4	1.4	0.1	0.3
	Na_2O			0.1			0.1	0.1					0.1	0.1	0.1	0.2	0.0	0.2	0.1	0.1
	Total			97.0			97.2	97.0					98.9	97.6	98.4	98.2	97.1	96.6	95.1	96.2
Hornblende	SiO_2	45.7	46.3	47.2	45.8	44.2	46.0	45.2	44.0	44.5	45.8	45.1	45.2	47.9	43.8	43.8	42.1	44.1		
	Al_2O_3	14.2	13.9	10.5	14.2	15.9	13.5	16.4	15.4	13.9	13.8	14.2	12.5	10.7	12.5	15.0	16.4	12.0		
	FeO	11.3	11.4	7.8	10.8	12.3	14.2	12.9	15.4	15.8	14.7	14.8	15.6	13.2	20.3	18.5	19.6	20.2		
	MnO	0.2	0.2	0.3	0.2	0.2	0.2	0.2	0.5	0.5	0.4	0.3	0.4	0.3	1.9	0.3	0.1	0.3		
	MgO	15.6	14.8	18.0	15.5	13.7	13.3	12.3	11.8	12.2	13.3	12.8	12.7	12.9	10.4	9.1	9.3	9.3		
	CaO	10.4	10.6	12.4	10.3	10.9	10.1	10.1	10.0	10.2	10.0	10.2	10.9	10.9	10.4	9.9	10.3	9.0		
	Na_2O	1.7	1.5	1.4	1.9	1.6	1.3	1.4	1.4	1.6	1.7	1.9	1.7	0.9	0.4	2.0	0.8	1.9		
	Total	99.1	98.7	97.6	98.7	98.8	98.6	98.5	98.5	98.7	99.7	99.3	99.0	96.8	99.7	98.6	98.6	96.8		

Ions per 23 oxygens.

		N30C	N30B	N01A	I34B	J87D	QB27C 2B	QB27C 2A	155	T59B	6A9	K44C	K44E	498	Y23C	7E8B	Q795	7A8B	Y42B	I38A
Anthophyllite	Si	7.12	7.40		7.02	7.13	7.53	7.56	7.45	7.15	7.29	7.03							7.59	7.64
	Al	0.88	0.60		0.98	0.87	0.47	0.44	0.55	0.85	0.61	0.97							0.41	0.36
	Al	0.71	0.55		0.78	0.71	0.47	0.49	0.45	0.59	0.58	0.53							0.25	0.32
	Mg	4.28	4.31		4.03	4.04	4.11	4.04	3.97	3.78	3.81	3.81							3.41	3.30
	Fe	1.80	1.97		1.97	2.16	2.25	2.25	2.41	2.38	2.51	2.56							3.29	3.27
	Mn	0.05	0.05		0.06	0.03	0.06	0.06	0.11	0.15	0.09	0.07							0.06	0.07
	Ca	0.09	0.06		0.19	0.03	0.06	0.06	0.04	0.10	0.10	0.08							0	0
	Na	0.28	0.17		0.33	0.19	0.10	0.14	0.10	0.23	0.26	0.31							0.11	0.09
	fe	30.3	31.9		33.5	35.2	36.1	36.4	38.9	40.1	40.6	40.9								
	an	24.9	26.8		21.6	13.7	35.3	30.5	29.9	32.6	22.7	20.1								
Cummingtonite	Si			8.02			7.83	7.83					7.88	7.90	7.92	7.86	7.85	7.83	7.90	7.90
	Al			—			0.17	0.17					0.12	0.10	0.08	0.14	0.14	0.17	0.10	0.10
	Al			0.09			0.28	0.33					0.10	0.07	0.08	0.12	—	0.19	0.15	0.60
	Mg			4.52			4.12	4.09					3.92	3.96	3.78	3.61	3.63	3.32	3.54	3.43
	Fe			2.08			2.28	2.23					2.69	2.75	2.79	3.13	3.34	3.14	3.16	3.38
	Mn			0.09			0.06	0.06					0.09	0.11	0.28	0.07	0.04	0.07	0.07	0.07
	Ca			0.12			0.21	0.21					0.15	0.10	0.06	0.04	0.06	0.22	0.02	0.05
	Na			0.03			0.02	0.02					0.03	0.03	0.03	0.05	0.00	0.05	0.04	0.04
	fe			32.4			36.2	35.8					41.6	41.9	44.9	47.0	48.3	49.2	47.8	40.3
	an			81.7			88.7	88.7					84.8	79.6	68.9	45.3	100.0	79.6	36.0	62.3
Hornblende	Si	6.48	6.59	6.74	6.46	6.33	6.63	6.47	6.39	6.49	6.51	6.26	6.84	6.99	6.49	6.46	6.24	6.68		
	Al	1.52	1.41	1.26	1.54	1.67	1.37	1.53	1.61	1.51	1.49	1.74	1.16	1.01	1.51	1.54	1.76	1.32		
	Al	0.85	0.92	0.49	0.82	1.00	0.92	1.23	1.03	0.87	0.81	0.58	1.06	0.81	0.66	1.07	1.09	0.81		
	Mg	3.30	3.14	3.83	3.26	2.93	2.85	2.63	2.56	2.65	2.82	2.65	2.86	2.81	2.30	2.00	2.05	2.10		
	Fe	1.34	1.35	0.93	1.27	1.47	1.71	1.54	1.87	1.92	1.74	1.71	1.97	1.60	2.51	2.28	2.43	2.56		
	Mn	0.02	0.02	0.03	0.02	0.02	0.02	0.02	0.06	0.06	0.05	0.03	0.05	0.03	0.24	0.03	0.01	0.04		
	Ca	1.58	1.62	1.90	1.56	1.67	1.56	1.55	1.56	1.59	1.52	1.52	1.76	1.70	1.65	1.56	1.63	1.46		
	Na	0.46	0.41	0.38	0.53	0.45	0.35	0.38	0.38	0.45	0.46	0.52	0.49	0.25	0.11	0.57	0.21	0.56		
	fe	29.3	30.6	20.2	28.5	33.9	37.8	37.4	43.1	42.9	38.9	39.8	41.4	37.0	54.1	53.7	54.3	55.3		
	an	77.2	79.6	83.0	74.9	79.0	81.1	80.0	79.8	77.9	76.5	74.8	78.0	87.0	93.4	73.2	87.7	72.3		

[a] Cornelis Klein, Jr., analyst.
fe = 100 (Fe+Mn)/(Fe+Mn+Mg).
an = 100 Ca/(Na+Ca).

(*Continued from page 255*)

cummingtonite gneiss and hornblende amphibolite layer. Hornblende grain selected for analysis was several mm inside amphibolite layer and may not have been in contact with cummingtonite host grains. Hornblende and cummingtonite contain (100) and ($\bar{1}$01) exsolution lamellae identical to those in 7A8BX.

498—Partridge Formation. Medium-grained, finely layered hornblende-cummingtonite-biotite amphibolite. Both hornblende and cummingtonite contain extremely thin ($\bar{1}$01) lamellae. Cummingtonite contains faint (100) lamellae but hornblende apparently contains none. Hornblende has peculiar pale brown and blue-green color.

Y23C—Fine-grained, dark-gray quartz-cummingtonite-garnet-magnetite-hornblende schist with layers and lenses of very fine-grained garnet and quartz. High spessartine content of garnet is suggested by

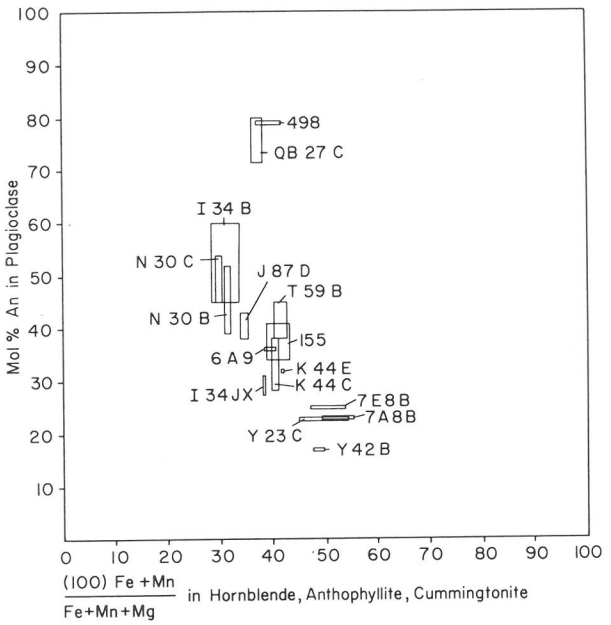

FIG. 2. Diagram showing 100(Fe + Mn)/(Fe + Mn + Mg) for amphiboles plotted against mole % An of coexisting plagioclase. Amphibole compositions determined by electron-probe or wet chemical analyses. Plagioclase compositions determined by measurement of α index of refraction in oils. Each box outlines observed composition range. Most specimens fall on an apparent igneous fractionation trend.

fine grain size and high MnO in both amphiboles. Both amphiboles contain ($\bar{1}01$) lamellae 0.25 μ thick and rare (100) lamellae about 0.20 μ thick.

7E8B—See 7E8BX

Q795—Partridge Formation, sillimanite zone, slightly retrograded, east shore of Little Quabbin Island, Windsor Dam quadrangle, Mass. Very coarse-grained garnet-plagioclase-cummingtonite-quartz-magnetite-hornblende gneiss with secondary hornblende and chlorite. Cummingtonite and some hornblende grains contain (100) and ($\bar{1}01$) lamellae 0.5 μ and 1.3 μ thick respectively.

7A8B—See 7A8BX

Y42B—Coarse-grained plagioclase-quartz-cummingtonite-anthophyllite gneiss. Trace of hornblende is probably secondary. No exsolution lamellae observed.

I38A—Same outcrop as I38DX but not described in detail elsewhere. Fine-grained, well bedded quartz-garnet-amphibole granulite. In a central layer about 2 cm thick the amphibole is cummingtonite. The boundary between the two mode areas in one thin section runs through this cummingtonite layer. On one side of this layer the cummingtonite is in contact with and intergrown with hornblende. In the vicinity of this contact the cummingtonite contains hornblende exsolution lamellae and has a few twins on (100). Crystals A, C-A, and 1 of Ross, Papike and Shaw, 1969, Table 6 are from near this contact. Crystal A, cummingtonite host, 90%; hornblende lamellae on (100), 6%; hornblende lamellae on ($\bar{1}01$), 4%, all space groups $C2/m$. Crystal C-A cummingtonite host, 98%; hornblende lamellae on (100), 2%; all $C2/m$. Crystal 1, hornblende host, 85%; cummingtonite lamellae on (100), 10%; cummingtonite lamellae on ($\bar{1}01$), 5%, all $C2/m$. On the other side of the cummingtonite layer cummingtonite is in contact with and intergrown with anthophyllite. Near this contact the cummingtonite is free of exsolution lamellae but is polysynthetically twinned on (100). The electron probe analyses of Klein (1968, see Fig. 14) and crystal 2 of Ross, Papike and Shaw are from near this contact. Anthophyllite host, 55%; submicroscopic gedrite exsolution, 45%, both *Pnma*. The high percentage of gedrite exsolution shown by the single crystal X-rayed is not consistent with the chemical composition given by the probe analysis, suggesting that anthophyllites of two different compositions were studied in this strongly layered rock.

Using the Frantz separator with a side slope of 12–15°, the intensity range at which optimum concentration of the amphiboles, described herein, occurs is as follows:

Anthophyllite	0.38–0.50 amp
Cummingtonite	0.33–0.45 amp
Hornblende	0.43–0.65 amp

In general, magnetic separation of anthophyllite from hornblende was relatively uncomplicated because members of coexisting pairs showed significant contrasts in their total Fe + Mn contents and relatively minor amounts of exsolution lamellae. On the other hand, magnetic separation of coexisting cummingtonite and hornblende proved to be extremely difficult because of smaller magnetic contrasts. Cummingtonites (or grunerites) richer in total Fe + Mn than those described herein have magnetic susceptibilities that overlap those of garnet and other ferromagnesian minerals to a degree where their magnetic separation becomes impossible.

The thirteen purified mineral samples for which complete chemical analyses are given in Table 2 were the product of most of two summers work by a full-time technician working under the direction of one of the authors. The purity of each of these samples and the amount recovered was as follows:

Sample No.	*Mineral*	*Amount Recovered (g)*	*Purity, %*
W95JX	Gedrite	3.6	99.8
I34JX	Gedrite	13.1	99.7
I34I	Gedrite	1.1	99.6
I38DX	Gedrite	25.1	99.4
N30X	Anthophyllite	7.5	99.8
6A9X	Anthophyllite	6.9	99.2
7E8BX	Cummingtonite	8.0	98.4
7A8BX	Cummingtonite	4.7	97.4
Y42BX	Cummingtonite	10.6	99.4
N30X	Hornblende	12.1	99.7
6A9	Hornblende	20.9	99.2
7E8BX	Hornblende	1.0	99.2
7A8BX	Hornblende	5.8	98.0

CHEMICAL INFERENCES ON ROCK ORIGIN

An interesting by-product of the amphibole analyses was the information they give concerning the origin of the plagioclase amphibolites. When the Fe/Fe + Mg ratios of the coexisting amphiboles are plotted against the optically determined composition range Ca/Na + Ca of the coexisting plagioclases (Fig. 2), a strong linear correlation is demonstrated with Na and Fe increasing sympathetically. Such a correlation would be expected in series of igneous rocks that differentiated by fractional crystallization of plagioclase and ferromagnesian minerals, and is supporting evidence that most of the plagioclase amphibolites are, in fact, metamorphosed volcanics.

CHEMOGRAPHIC RELATIONS

The graphical representation of amphibole compositions and assemblages has long been a major problem (Hallimond, 1943; Winchell, 1945; Colville et al., 1966; Ernst, 1968). The composition range and number of different substitutions is so great that attempts at describing compositions graphically remind one of the proverbial blind men

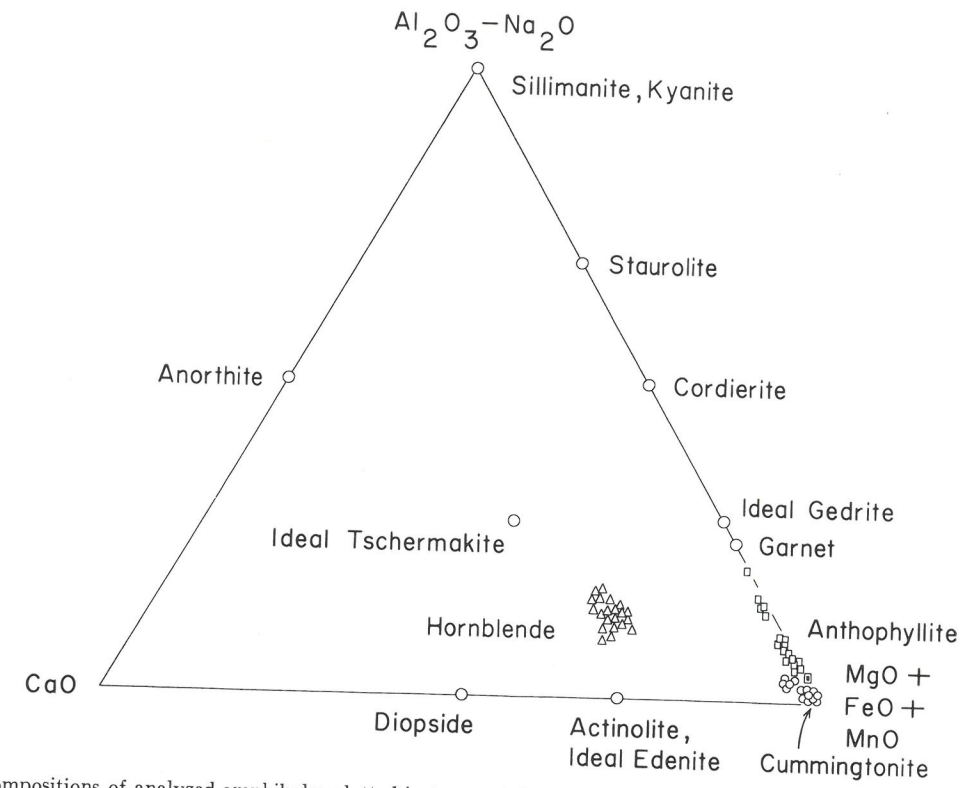

FIG. 3. Compositions of analyzed amphiboles plotted in terms of the components (Al_2O_3 — Na_2O), CaO, (FeO + MnO + MgO). Triangles, hornblende; squares, anthophyllite; circles, cummingtonite. Compositions of ideal amphibole end members and other minerals also shown.

describing an elephant. To describe common amphiboles to a first approximation the components SiO_2-Al_2O_3-Fe_2O_3-TiO_2-FeO-MnO-MgO-CaO-Na_2-H_2O are required. This list may be reduced to four, Al_2O_3, CaO, Na_2O, (FeO + MnO + MgO), at the apices of a tetrahedron by the following procedure:

1. Assume SiO_2 is present in excess as the phase quartz. This assumption is valid for many specimens but not all.
2. Ignore the important crystal-chemical differences between MgO, FeO, and MnO.
3. Ignore Fe_2O_3 and TiO_2.
4. Treat H_2O as a perfectly mobile component controlled by the activity of H_2O of the environment.

By ignoring coupled Na/Na substitution in the *A* and *M*(4) sites as in richterite, and assuming further that all Na substitution is compensated by Al either in four-coordination as in edenite or in six-coordination as in glaucophane, it is possible to represent the investigated amphibole compositions in terms of the three components (Al_2O_3-Na_2O), CaO, (FeO + MnO + MgO) at the apices of a triangle (Fig. 3). The assumption of no Na/Na substitution is reasonable for the Orange area rocks because these are relatively Al-rich. Because of the components chosen, this diagram portrays coupled Al/Al substitution in six- and four-coordination more or less completely, but not Na/Al substitution, hence ideal edenite or glaucophane appear at the base. In addition to the analyzed amphiboles and ideal end-member amphibole compositions, the compositions of a number of other coexisting phases may be shown. Since all of the amphibole compositions fall in the portion near the apex FeO + MnO + MgO, this portion is used in enlarged form for detailed examination of composition relations (Fig. 4) leading to the observations summarized below.

In the case of the wet analyses further refinements are possible by taking into account Fe_2O_3, TiO_2 and Cr_2O_3 which are presumed to go into octahedral positions compensated by tetrahedral Al according to the scheme $[Fe^{3+}, (Fe^{2+}Ti^{4+})_{1/2}, Cr^{3+}]/Al^{3+}$. These oxides may be added to Al_2O_3 to portray the total amount of octahedral-tetrahedral substitution (R^{3+}/Al^{3+}), or an amount of Al_2O_3 equivalent to these oxides can be subtracted so that the remaining Al_2O_3 portrays strictly Al/Al substitution. The latter method is particularly important if octahedral Al, as distinct from octahedral Fe^{3+} and Ti^{4+} is favored by high pressure (Thompson, 1947; Leake, 1965; Binns, 1965). Both of these methods were tried to adjust the compositions shown in Figure 4E, but the results are not given here because neither drastically alters the topologic relations shown.

Al/Al substitution. Hornblendes coexisting with anthophyl-

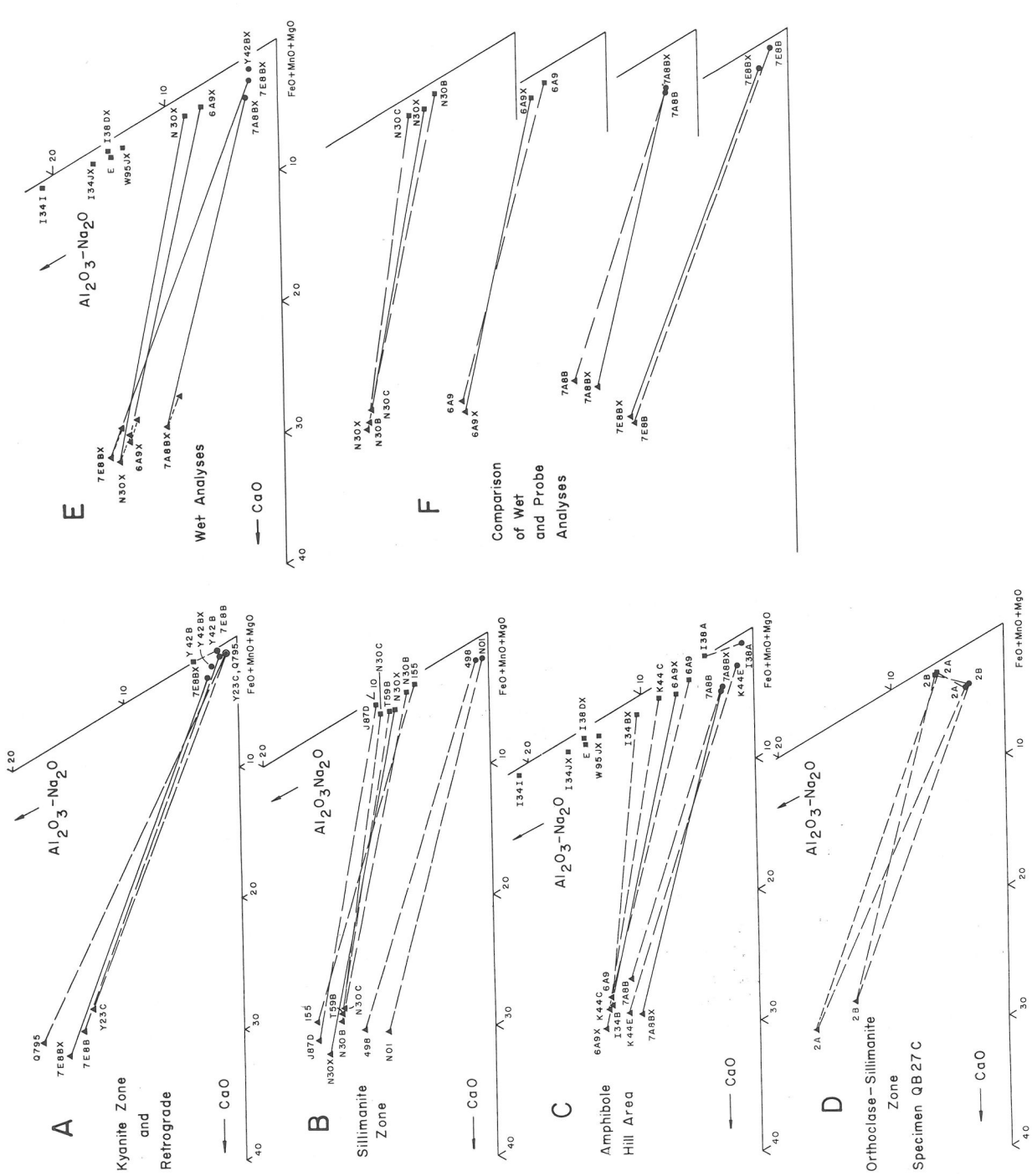

FIG. 4. Detailed composition relations of amphiboles in the FeO + MnO + MgO corner of the triangle (Al_2O_3 — Na_2O), CaO, (FeO + MnO + MgO). A, B, C, D. Solid lines, wet analyses; dashed lines, probe analyses. E. Solid lines, wet analyses; dashed lines connect wet analyses of hornblendes with same analysis with total Fe as FeO. F. Solid lines, wet analyses with total Fe as FeO; dashed lines, probe analyses.

lite or cummingtonite and plagioclase are very high in Al/Al substitution. Al/Al is lower in hornblendes coexisting with cummingtonite from the sillimanite zone (498, K44E, 7A8B) than it is in hornblendes coexisting with cummingtonite from the kyanite zone (7E8B, Y23C) or retrograded specimens (Q795). This is in close agreement with the prograde reaction tschermakitic hornblende + quartz→less tschermakitic hornblende + cummingtonite + plagioclase + H_2O proposed by Shido (1958). The low Al hornblende in specimen NO1A occurs in an ultramafic rock containing no plagioclase.

Anthophyllites coexisting with hornblende contain high Al/Al substitution, but less than the hornblende. Anthophyllites coexisting with cordierite (W95JX, I34JX), aluminum silicates (I34I), or garnet (I38DX) contain more Al than anthophyllites with hornblende. The diagrams suggest that low Al anthophyllite would not be found with plagioclase under these metamorphic conditions, but only in metamorphosed ultramafic or peculiar sedimentary rocks. Further, the high Mg content of cummingtonite in ultramafic rock NO1A suggests the cummingtonite field may extend to considerably higher Mg content in plagioclase-free than in plagioclase-bearing rocks. The association of cummingtonite and plagioclase in magnesian rocks is apparently cut out by the association of anthophyllite and hornblende.

Cummingtonites coexisting with hornblende have low Al/Al and Ca substitution, and what they do show is now largely in the form of hornblende exsolution lamellae. In the analyzed anthophyllite-cummingtonite pairs (Y42B, I38A, QB27C) the anthophyllite is richer in Al, and there is no compositional overlap of anthophyllite and cummingtonite even though MgO, FeO, and MnO are treated as one component.

In Figure 4F wet and probe analyses of four amphibole pairs are compared directly. The wet analyses are shown with total Fe as FeO for direct comparison with probe analyses. It was hoped that this comparison would show a more closed miscibility gap in the wet pairs as compared to the probe pairs, but this is realized only for specimen 7E8B. The absence of this relation in the other pairs is an indication of how slight the amount of coarse exsolution was during the late metamorphic history of the Orange area. This is in sharp contrast to amphibole pairs from the Ruby Mountains, Montana (Ross, Papike, and Shaw, 1969, this volume).

Na substitution. By ignoring Al_2O_3 it is possible to relate amphibole compositions to optically determined plagioclase compositions using the triangle $NaO_{1/2}$, CaO, (FeO + MnO + MgO) (Fig. 5). This shows that the Na content of hornblende is relatively insensitive to variation in the Na content of coexisting plagioclase. There seems to be some inherent crystal-chemical limit on the Na content of hornblende that is less than the theoretical edenite end member. Thus, hornblendes with oligoclase, andesine, and labradorite all seem to have about the same Na content (see also Leake, 1965). However, hornblendes coexisting with bytownite (498, QB27C) are lower in Na, and there is less Na in hornblende in essentially plagioclase-free rocks (NO1A, Y23C).

In order to show details of amphibole composition the FeO + MnO + MgO corner of the triangle is shown in greater detail in Figure 6. A surprising conclusion from Figure 6 and from Table 2 is that anthophyllites coexisting with hornblende contain abundant Na, about half as much as coexisting hornblende. Furthermore anthophyllites with cordierite (W95JX, I34JX), aluminosilicates (I34I), or garnet (I38DX) equal or surpass hornblende in Na content. This leads to speculation on the structural position of Na in anthophyllite. Na in $M(4)$ positions as in glaucophane is unlikely because small ions in $M(4)$ seem required to stabilize the orthorhombic amphibole structure. Substitution of Na in A positions seems likely, and would be enhanced by the very high Al in adjacent tetrahedral sites. The most sodic anthophyllite, I34I (also the most aluminous), contains 0.537 Na per 24 O(OH) equivalent to a filling of ½ of the A sites if all Na is in A. The most sodic hornblende, 7E8BX (also close to the most aluminous), contains 0.584 Na per 24 O(OH). A complete structural formula for anthophyllite I34I (Table 6) suggests that 0.325 Na is in A and 0.212 in $M(4)$, but this site assignment assumes that the excess H_2O in the analysis is substituted as 0.58 (OH) for O. If, on the other hand, the excess H_2O is accounted for as H_4O_4 tetrahedra substituting for SiO_4, then the Na content assigned to A would be higher.

The apparent correlation between high Na and high Al in both anthophyllites and hornblendes was explored further in a diagram (Fig. 7) showing Na + K per 24 $O(OH)$ plotted against Si per 24 $O(OH)$ (or 23 O in the case of probe analyses) (Hallimond, 1943; Leake, 1968; see also Dodge *et al.*, 1968, Fig. 12). This presentation has the advantage of showing both Na/Al substitution and R^{3+}/Al substitution, and includes compositions of several ideal end members. Since it portrays only tetrahedral occupancy, it is immaterial whether the coupled octahedral cations are Al^{3+}, Fe^{3+}, $Fe^{2+}Ti^{4+}$, or Cr^{3+}. Nearly all of the analyzed amphiboles reported here plot in a linear group trending from the origin to about $(Na+K)_{0.6}Si_6$. The anthophyllites in particular show a tight linear trend. Most of the hornblendes are slightly more sodic. Three possible explanations for the linear trend are considered: (1) limited bulk composition of specimens studied; (2) limited conditions of metamorphism of specimens studied; (3) something in the crystal chemistry of both amphibole groups. The first explanation can probably be discounted on the basis of the wide variety of bulk compositions reported here alone, although no hornblendes from calc-silicate rocks are included. The second explanation was tested by comparing this plot with that of a suite of hornblendes from the Sierra Nevada batholith (Dodge, Papike, and Mays, 1968, Fig. 12), hornblendes from volcanic glass

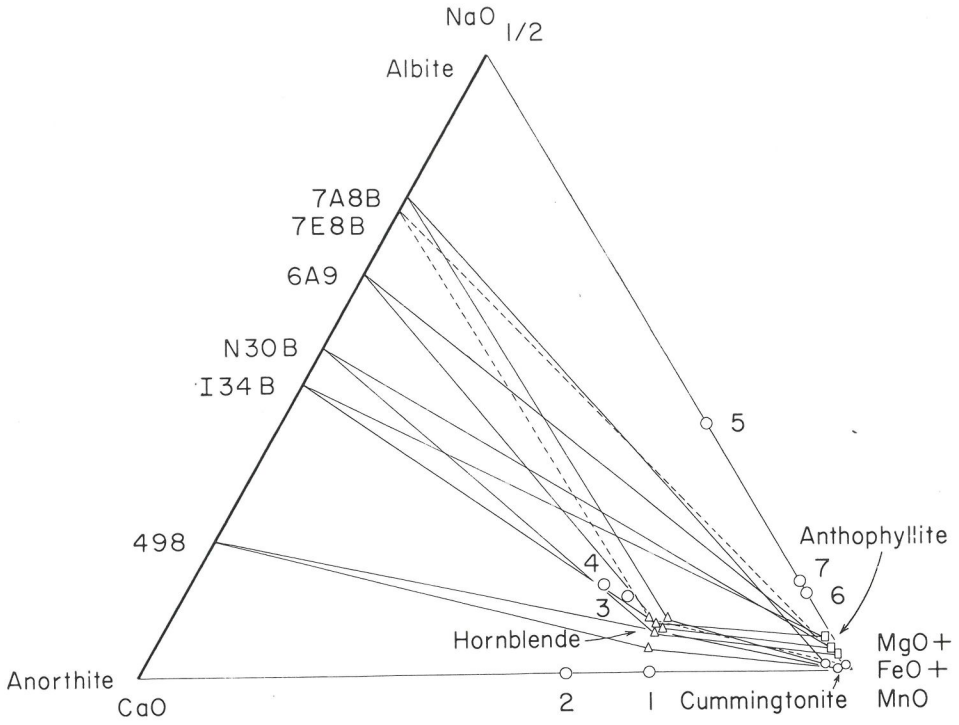

FIG. 5. Compositions of coexisting amphiboles and plagioclases plotted in the triangle $NaO_{1/2}$, CaO, (FeO + MnO + MgO). Solid lines, sillimanite zone; dashed lines, kyanite zone assemblage. Ideal amphibole end-member compositions:

1. $\circ Ca_2(Mg,Fe)_5Si_8O_{22}(OH)_2$	Actinolite
2. $\circ Ca_2Mg_3Al_2Al_2Si_6O_{22}(OH)_2$	Tschermakite
3. $NaCa_2Mg_5AlSi_7O_{22}(OH)_2$	Edenite
4. $NaCa_2Mg_4AlAl_2Si_6O_{22}(OH)_2$	Pargasite
5. $\circ Na_2Mg_3Al_2Si_8O_{22}(OH)$	Glaucophane
6. $NaMg_7AlSi_7O_{22}(OH)_2$	
7. $NaMg_6AlAl_2Si_6O_{22}(OH)_2$	

(Klein, 1968), and hornblendes from sillimanite zone and granulite facies metamorphic rocks from New South Wales (Binns, 1965). All fall within the same area on the diagram. Thus some crystal-chemical factor relating *A* site occupancy to tetrahedral Al occupancy in a ratio of about 1:3 seems the most probable explanation. Although the Sierra, New South Wales, and the Orange area hornblendes are grouped on the basis of Na and Si, they differ in their compensating octahedral ions as follows:

	Octahedral Al		Octahedral $Fe^{3+}+2Ti^{4+}+Cr^{3+}$	
	Median	Range	Median	Range
Seirra Nevada Hornblendes	0.26	0.13–0.53	0.68	0.44–0.91
N.S.W. Hornblendes, Granulite Facies	0.37	0.33–0.45	0.74	0.51–0.92
N.S.W. Hornblendes, Sillimanite-Orthoclase Zone	0.55	0.47–0.63	0.58	0.33–0.64
N.S.W. Hornblendes, Sillimanite-Muscovite Zone	0.66	0.54–0.80	0.74	0.49–0.86
Orange, Hornblendes	0.69	0.42–0.77	0.58	0.54–0.77
Orange, Anthophyllites	0.90	0.41–1.25	0.19	0.17–0.36

Furthermore there is a strong difference between the Orange area hornblendes and anthophyllites. In the case of the New South Wales hornblendes, Binns has demonstrated that most of the differences in compensating octahedral ions are a function of metamorphic grade.

Cummingtonites with either hornblende or anthophyllite contain negligible Na and their Ca is now largely expressed in exsolved hornblende lamellae. Even on the finest scale (Fig. 8) anthophyllites and cummingtonites can be discriminated on the basis of their Na contents and Na/Ca ratios.

Mg-Fe Substitution. In order to examine the different roles of MgO and FeO it is necessary to expand the number of components to treat these two separately. They may be combined with CaO to form the triangle CaO, MgO, FeO in which appears an "Amphibole Quadrilateral" (Ross, Papike, and Weiblen, 1968; Klein, 1968, Fig. 3) analogous to the familiar "Pyroxene Quadrilateral". This procedure has one serious drawback; it completely obscures the important role of Al/Al substitution in the hornblende and anthophyllite. Since this Al/Al substitution is best shown in the triangle (Al_2O_3-Na_2O), CaO, (FeO + MnO + MgO), this triangle can be expanded to form a tetrahedron (Al_2O_3-Na_2O), CaO, MgO, (FeO + MnO) (Fig. 9). Tie-

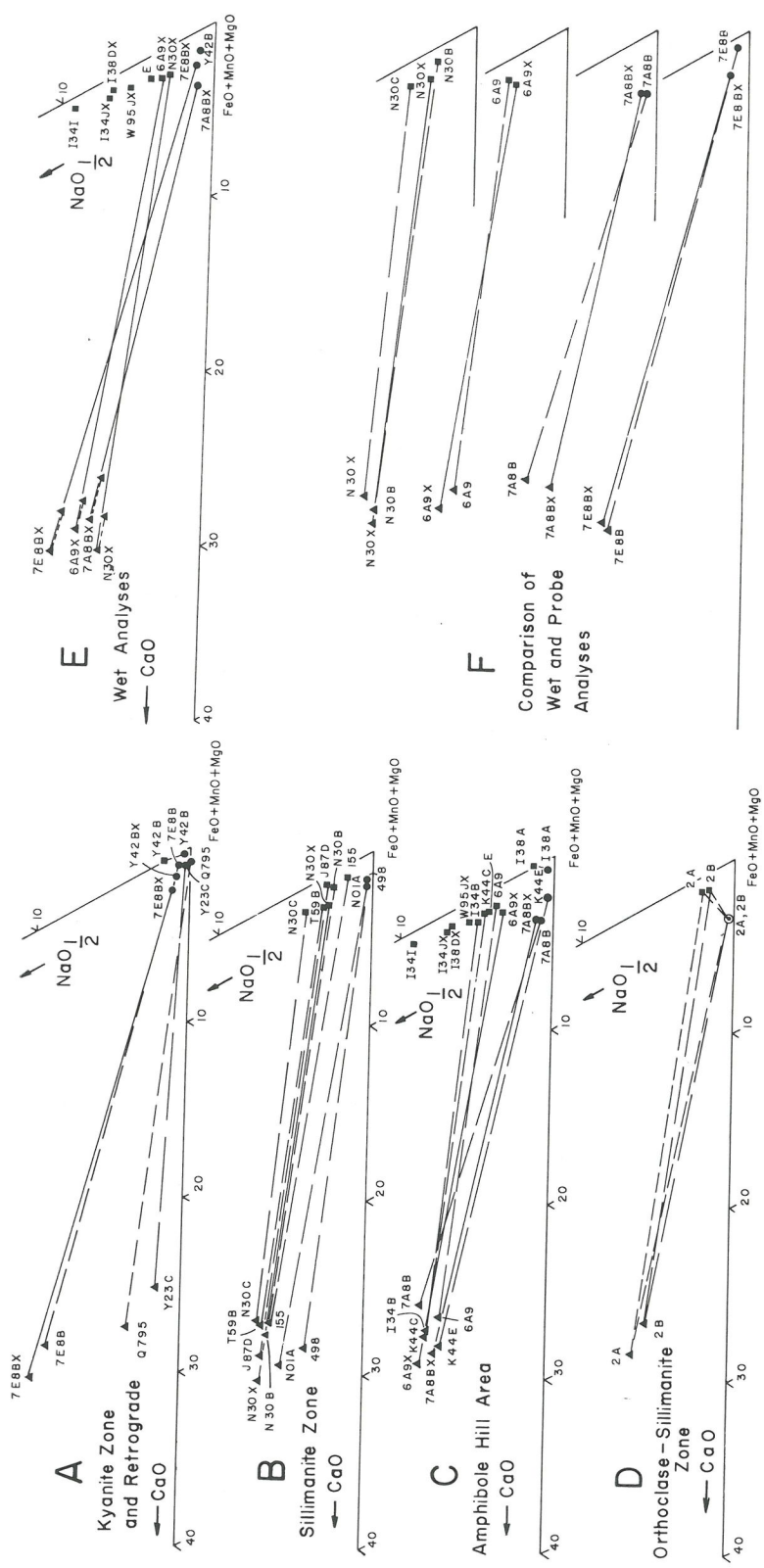

FIG. 6. Detailed composition relations of amphiboles in the FeO + MnO + MgO corner of the triangle $NaO_{1/2}$, CaO, (FeO + MnO + MgO). A, B, C, D. Solid lines. wet analyses; dashed lines, probe analyses. E. Solid lines, wet analyses; dashed lines connect wet analyses to same analyses with total Fe as FeO. F. Solid lines, wet analyses with total Fe as FeO; dashed lines, probe analyses.

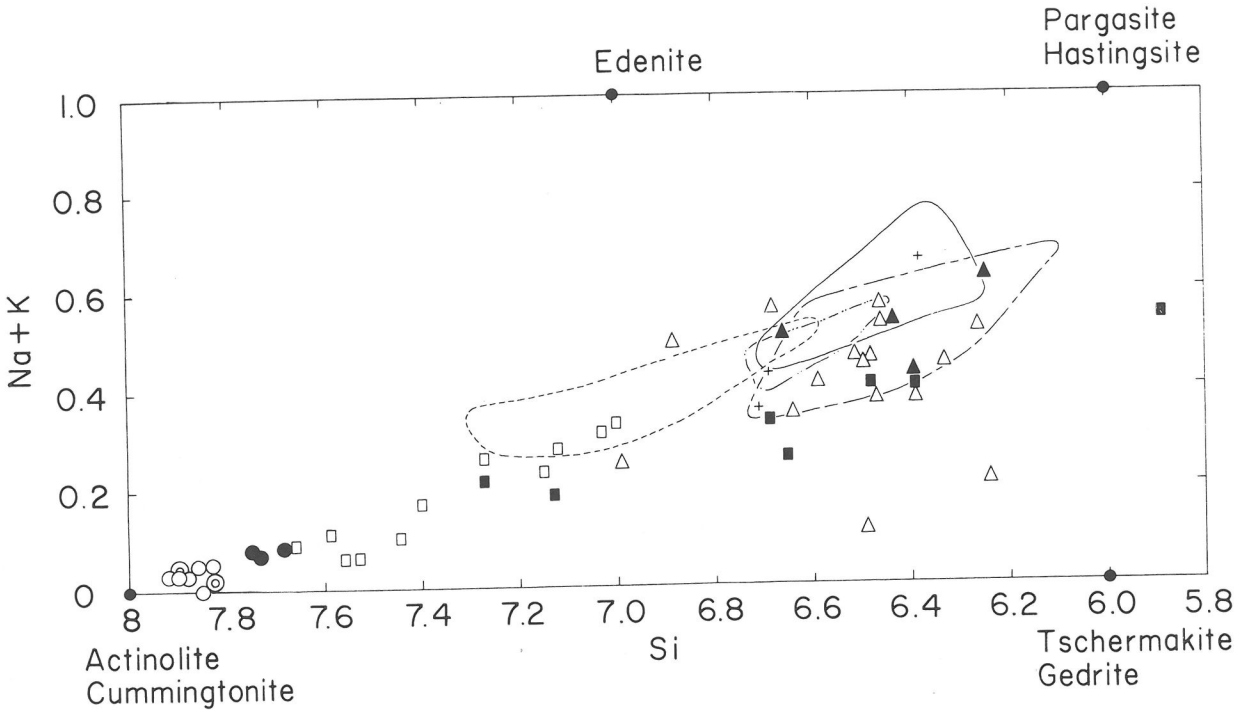

FIG. 7. Plot of Na + K versus Si atoms per formula unit for analyzed amphiboles from the Orange area and adjacent areas. Symbols: Triangles, hornblende; squares, anthophyllite; circles, cummingtonite; closed symbols, wet analyses; open symbols, probe analyses; crosses, hornblendes from volcanic glass (Klein, 1968). Lines outline fields of analyzed hornblendes from the Sierra Nevada batholith (Dodge *et al.*, 1968) and from three metamorphic zones in New South Wales (Binns, 1965): short dashed-Sierra Nevada; solid-N.S.W. granulite facies; dash dot-N.S.W., amphibolite facies, sillimanite-orthoclase zone; long dash-N.S.W., amphibolite facies, sillimanite-muscovite zone.

line orientations in such a tetrahedron are best seen by some sort of projection from the composition of an ubiquitous phase as shown by Thompson (1957). For this study the composition of anorthite was chosen as the projection point (see also Green, 1960). The resulting projections of assemblages are true phase diagrams only if the following requirements are fulfilled: (1) the assemblage contains quartz, (2) the assemblage contains plagioclase, (3) the plagioclase composition has no influence on the amphibole compositions, and (4) other components are negligible. These requirements are probably rarely fulfilled, but the projections nevertheless prove useful for comparing assemblages.

Two different planes have been used for projection from the anorthite point. The projection plane CaO, MgO, (FeO + MnO) (Fig. 9) has the advantage of easy comparison with the amphibole and pyroxene quadrilaterals (see Robinson, Jaffe, Klein, and Ross, 1969, Fig. 2). Al/Al substitution in anthophyllite shows as a negative quantity of CaO. Cummingtonites fall close to the MgO, (FeO + MnO) line, showing neither positive nor negative CaO.

The other projection plane, (Al_2O_3-Na_2O), MgO, (FeO + MnO), is adopted here (Fig. 10). It has several advantages. The compositions of anthophyllite, cummingtonite, cordierite, staurolite, garnet, kyanite and sillimanite are on or close to the plane and their Al_2O_3, MgO, and (FeO + MnO) contents are shown directly. The excess CaO over (Al_2O_3-Na_2O) in hornblende plots as a negative value of Al_2O_3. Cummingtonites again fall very close to the MgO, (FeO + MnO) line, with neither positive nor negative amounts of Al_2O_3.

The most useful property of this projection, shown in enlarged form in Figure 11, is that it outlines all of the field of anthophyllite coexisting with quartz and plagioclase, including both aluminous assemblages and hornblende-bearing assemblages. This is best seen in the diagram showing analyses from "Amphibole Hill" (Fig. 11C) and in a generalized form in Figure 12. On the high Al side of the anthophyllite field, anthophyllite coexists with cordierite, aluminum-silicate or staurolite depending on the Fe/Mg ratio. Al is less in magnesian anthophyllite with cordierite (W95JX, I34JX) than in more Fe-rich anthophyllite with sillimanite and staurolite (I34I). On the high Fe limit of the anthophyllite field, not well known in detail, anthophyllite coexists with pyrope-bearing almandine and cummingtonite or staurolite. On the low Al side of the anthophyllite field, anthophyllites with (100) Fe/(Fe + Mg) = 41 or less coexist with hornblende (I34B, 6A9, K44C), and more Fe-rich anthophyllites coexist with cummingtonite (I38A). The anthophyllite with the lowest Al content coexists with

TABLE 6. ALTERNATIVE STRUCTURAL FORMULAE FOR ANTHOPHYLLITE I34I

I			II		
K	0.007	0.332	K	0.007	0.478
Na	0.325		Na	0.471	
Na	0.212		Na	0.066	
Ca	0.042		Ca	0.042	
Fe^{2+}	2.326		Fe^{2+}	2.326	
Mg	2.967		Mg	2.967	
Mn^{2+}	0.030	7.00	Mn^{2+}	0.030	7.00
Fe^{3+}	0.132		Fe^{3+}	0.132	
Cr^{3+}	0.002		Cr^{3+}	0.002	
Ti^{4+}	0.027		Ti^{4+}	0.027	
Al	1.245		Al	1.391	
Al	2.121		Al	1.975	
Si	5.874	8.00	Si	5.874	8.00
P	0.005		P	0.005	
			H_4	0.146	
O	21.417	22.00			
(OH)	0.583		O_{22}		
(OH)	1.995	2.00	(OH)	1.995	2.00
F	0.005		F	0.005	

cummingtonite and has nearly the same Fe/Mg ratio as the cummingtonite.

Cummingtonites coexisting with hornblende and plagioclase have (100) Fe/(Fe + Mg) as low as 41.5 (Table 4). One hornblende-cummingtonite rock without plagioclase (NO1B) has cummingtonite with (100) Fe/(Fe + Mg) of only 32. It is suggested that in the presence of plagioclase this pair would react to form a hornblende-anthophyllite assemblage under the metamorphic conditions of the area.

The evaluation of Fe/Mg ratios of coexisting amphiboles analyzed by electron probe is difficult because the probe analyses do not show the ferric iron content. Clearly the tie-line orientations of hornblende assemblages based on probe analyses (Fig. 11) are inconsistent with each other and with what is known of analogous pyroxene assemblages. The wet analyses (Table 2, Fig. 11E) show that one fifth to nearly one half of the Fe in hornblende is Fe^{3+}, anthophyllite has much less Fe^{3+}, and cummingtonite has still less. The anthophyllites have a higher FeO/MgO ratio than coexisting hornblendes as might be expected by analogy with analyzed coexisting hypersthene and augite (Kretz, 1963). In the probe analyses of coexisting hornblende and cummingtonite, the high total Fe in the hornblende is probably due to high Fe^{3+} in hornblende. This together with probably low Fe^{3+} in cummingtonite results in a peculiar tie-line orientation. In the wet analyses cummingtonite has about the same FeO/MgO ratio as the hornblende.

Based on probe analyses of hornblende and anthophyllite (K44C), and hornblende and cummingtonite (K44E) in the same outcrop in the "Amphibole Hill" area, a stable three-amphibole assemblage should occur at a ratio of (100) Fe/(Fe + Mg) = 41. Several three-amphibole specimens were found in the Orange area, but in each case the third amphibole is minor and possibly secondary. A true equilibrium three-amphibole assemblage was long sought. In 1965 such a specimen was found in the Quabbin Reservoir area in a zone of higher grade metamorphism characterized by the association of quartz, sillimanite, and orthoclase in mica schists. This specimen, QB27C, described in greater detail elsewhere (Robinson, Jaffe, Klein, and Ross, 1969), contains primitive cummingtonite with hornblende exsolution lamellae, hornblende with primitive cummingtonite lamellae, and anthophyllite that appears optically homogeneous but is a submicroscopic intergrowth of anthophyllite and gedrite. Two sets of electron-probe analyses near two mutual three-amphibole contacts are given in Table 4 and portrayed on Figures 4D, 6D, and 11D. Hornblende and cummingtonite analyses 2B are of material full of exsolution lamellae that were probably included in the analysis areas, hence the analyses probably come fairly close to representing the bulk composition of the grains prior to exsolution. Hornblende analysis 2A is of more tschermakitic material free of lamellae that is probably a product of retrograde reaction with the bytownite matrix during or after exsolution. Its composition plotted on Figure 4D shows clearly that it cannot be considered merely as a hornblende from which exsolved primitive cummingtonite has been removed.

The high Mg content of the primitive cummingtonite [(100) Fe/(Fe+Mg) = 36] as compared to the cum-

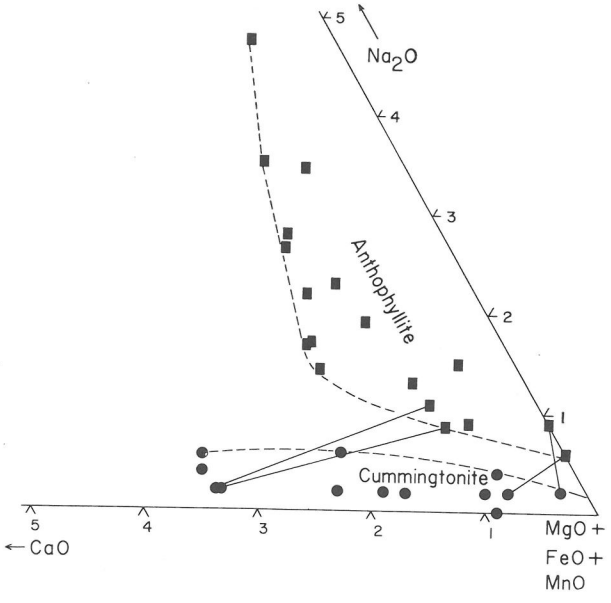

FIG. 8. Na_2O and CaO contents of anthophyllites and cummingtonites expressed in a portion of the triangle Na_2O, CaO, (FeO + MnO + MgO). Na_2O rather than $NaO_{½}$ is used here to give diagram a more equant shape.

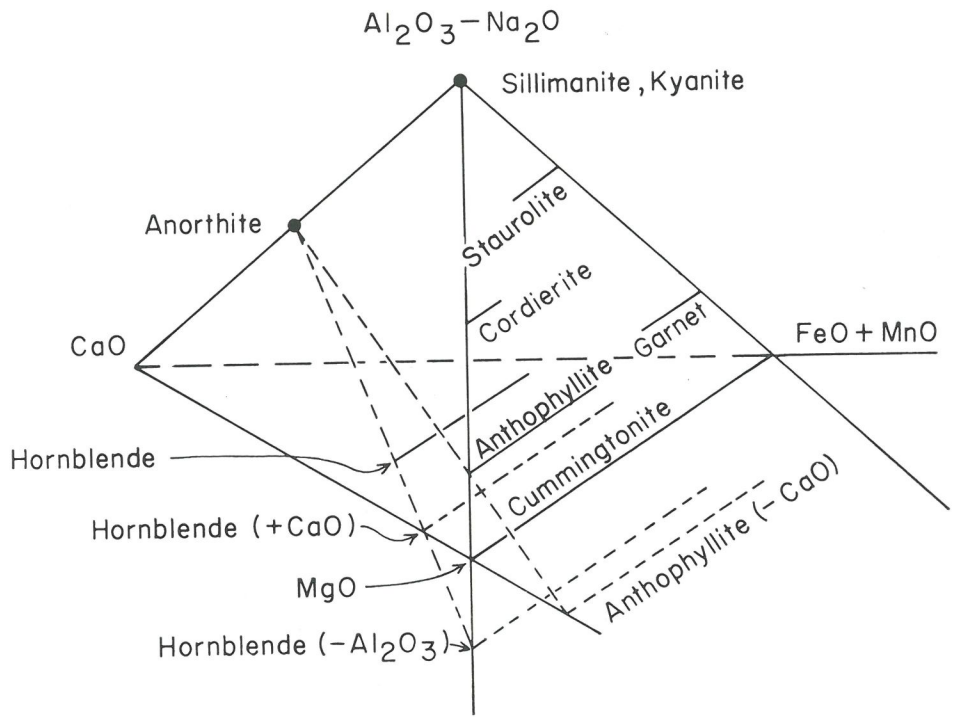

FIG. 9. The tetrahedron ($Al_2O_3 - Na_2O$), CaO, MgO, (FeO + MnO) showing the two planes used for projection from the anorthite point; CaO, MgO, (FeO + MnO) and ($Al_2O_3 - Na_2O$), MgO), (FeO + MnO).

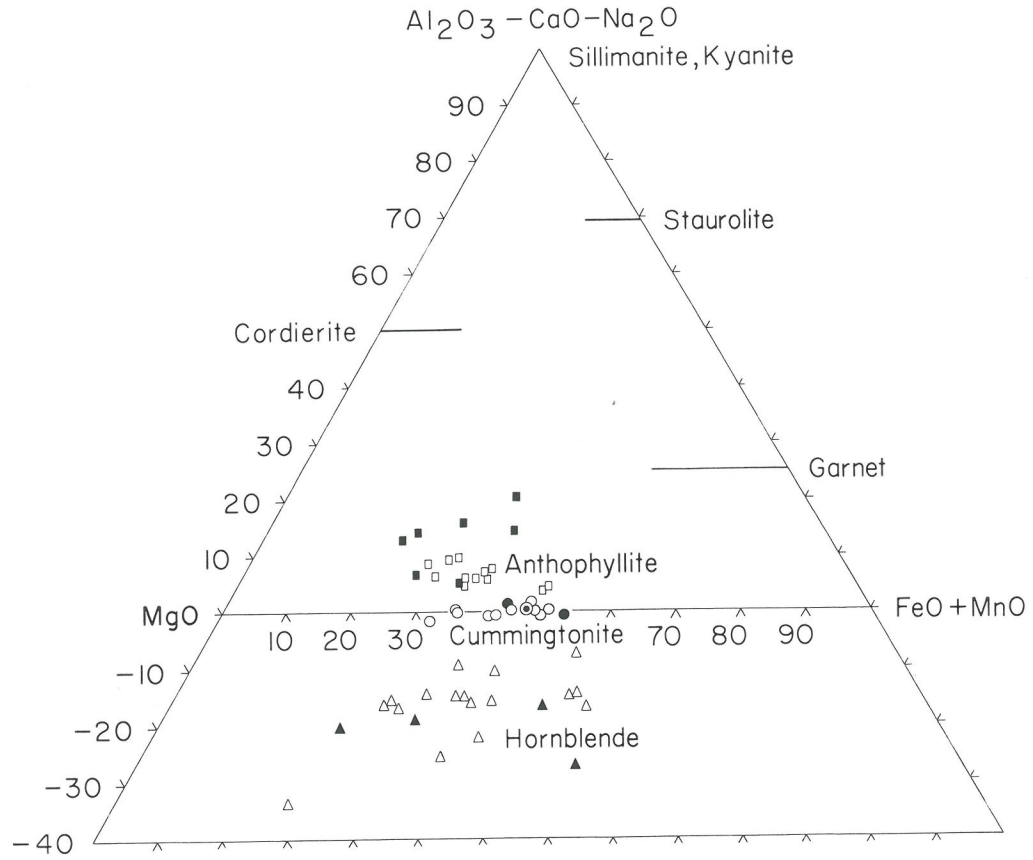

FIG. 10. Compositions of analyzed amphiboles (projected from plagioclase) on the plane ($Al_2O_3 - CaO - Na_2O$), MgO, (FeO + MnO). Closed symbols, wet analyses; open symbols, probe analyses.

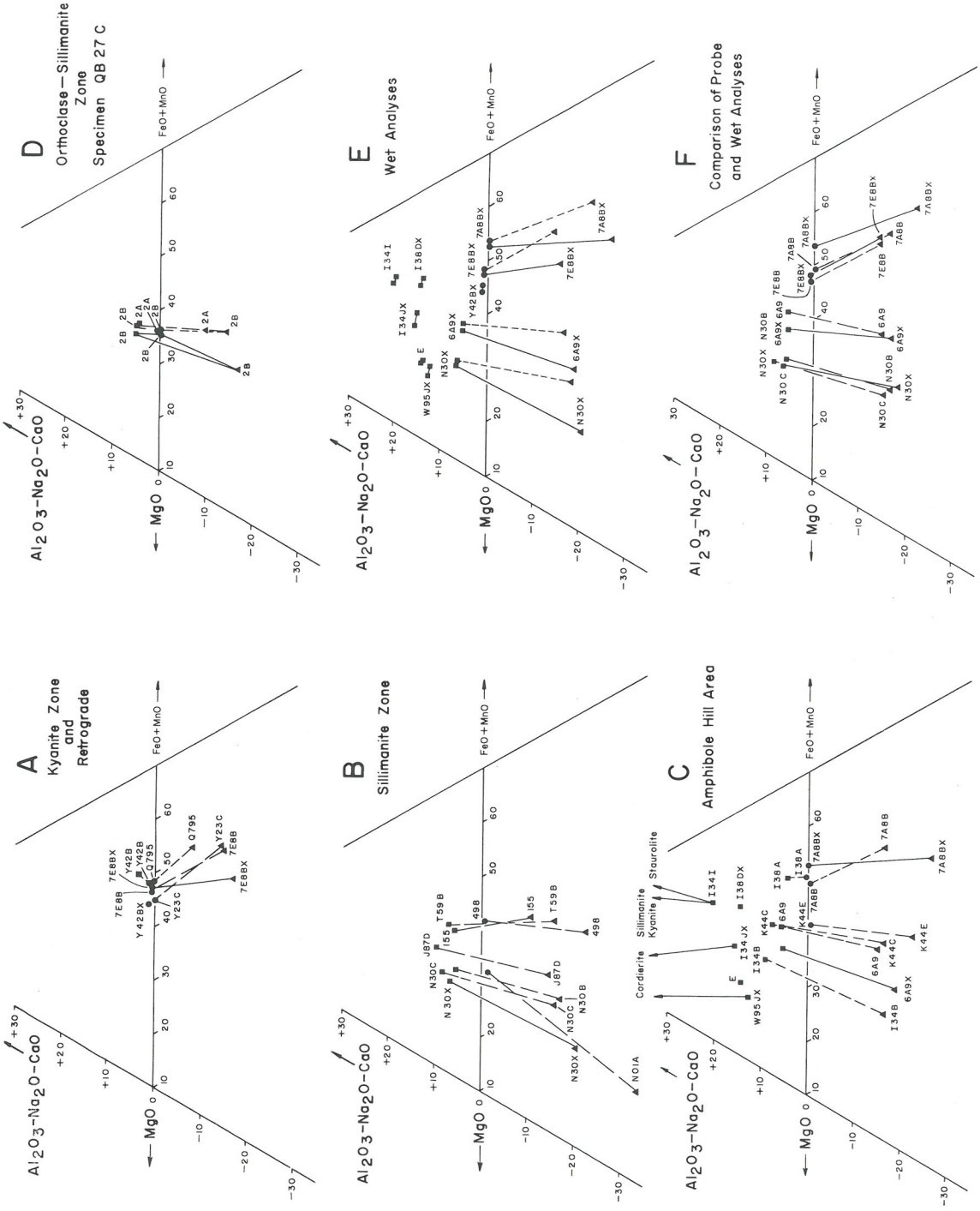

FIG. 11. Detailed composition relations of amphiboles in a portion of the projection ($Al_2O_3 - Na_2O - CaO$), MgO, (FeO + MnO). A, B, C. Solid lines, wet analyses; long dashed lines, probe analyses. D. Dashed lines, probe analyses: solid lines, probe analyses with inferred ferric corrections. E. Solid lines, wet analyses; dashed lines, wet analyses recalculated with total Fe as FeO; dashed lines, probe analyses,

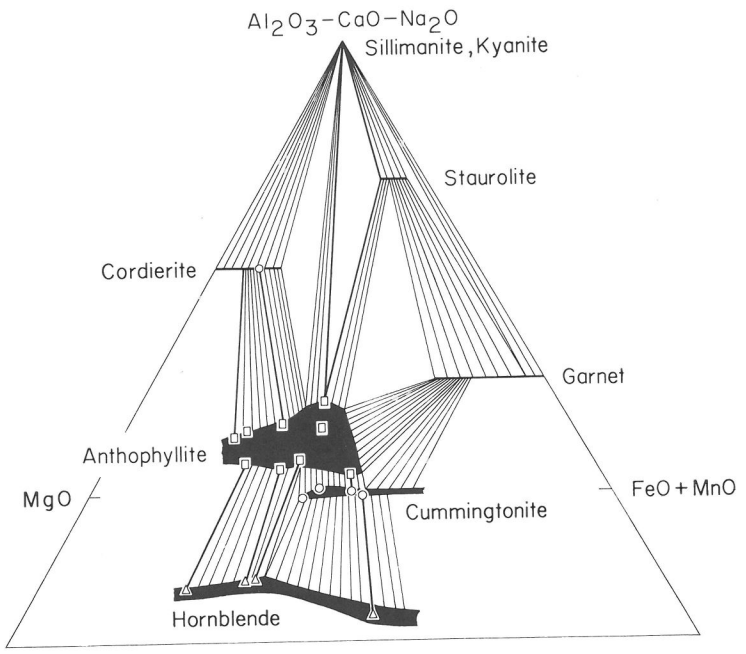

FIG. 12. Generalized topology of the projection (Al_2O_3 — CaO — Na_2O), MgO, (FeO + MnO) representative of the mineral facies of the "Amphibole Hill" area. The boundaries of the anthophyllite field are shown as well as a compositionally narrow region in which anthophyllite, cummingtonite and hornblende can coexist stably.

mingtonite from the hypothetical three-amphibole assemblage of the Amphibole Hill area [(100) Fe/(Fe+Mg) = 41] suggests a possible prograde reaction: Hornblende + anthophyllite + quartz→cummingtonite + plagioclase + H_2O, in which the cummingtonite becomes progressively more Mg-rich at the expense of the other two amphiboles. The hornblende and anthophyllite contribute their Na, Ca, and Al to plagioclase which becomes more Ca-rich, at least until obtaining the same Na/Na + Ca ratio as the hornblende. Since all of the octahedral Al in the hornblende and anthophyllite becomes tetrahedral in plagioclase, a considerable increase in entropy results. Theoretically, where the three amphiboles, quartz, and plagioclase coexist at arbitrarily chosen P and T, for each cummingtonite Fe/Mg ratio there should be a particular plagioclase. In practice the cummingtonite compositions in this critical assemblage probably do not change widely, whereas the plagioclases probably do.

METAMORPHIC FACIES OF CA-POOR ASSEMBLAGES

Rock compositions on the CaO-free face of the tetrahedron (Al_2O_3-Na_2O), CaO, MgO, (FeO + MnO) are rare but sufficiently abundant worldwide to allow recognition of several different metamorphic facies. The facies of the "Amphibole Hill" area is summarized in Figure 13A. The critical assemblage quartz-anthophyllite-kyanite-staurolite of specimen I34I is also described in detail by Hietanen (1959) from Idaho, and by Tilley (1939) from the Shueretsky District, Kola, U.S.S.R. Both the "Amphibole Hill" and Idaho specimens contain sillimanite coexisting with kyanite. Even though the assemblage quartz-cordierite-anthophyllite-sillimanite in the strict sense is not identified at "Amphibole Hill," cordierite-rimmed enclaves of sillimanite and kyanite in anthophyllite rock (I34JX) indicate at least passing stability in the course of progressive formation of cordierite from former sillimanite- (and kyanite) anthophyllite rock (Robinson and Jaffe, 1969).

At Pistil Ogo, the Lizard, Cornwall, Tilley (1937) describes two different assemblages: quartz-anthophyllite-cordierite-staurolite and quartz-andalusite-cordierite-staurolite (Fig. 13B). Tilley notes "Andalusite and anthophyllite are never found in close association. If they occur together in a single thin section they are relegated to different bands. They are clearly incompatible." Similar assemblages with sillimanite instead of andalusite have been described by Butler (1964) in rocks some distance beneath the Stillwater Complex in Montana. The quartz-andalusite-cordierite-staurolite assemblage is also reported by Zwart (1962) in the Pyrenees and Chinner (1966) in northeastern Scotland.

At Trelease Mill and Polkernogo, also on the Lizard. Tilley (1937) reports granulites containing the assemblage quartz-cordierite-cummingtonite-oligoclase in some of which cummingtonite is associated with anthophyllite in parallel growth. Tilley writes "In these intergrowths cummingtonite forms the core of the composite prism with a shell of anthophyllite." In some cordierite-anthophyllite rocks from Träskböle in the Orijärvi District, Eskola (1914) describes small amounts of cummingtonite, again

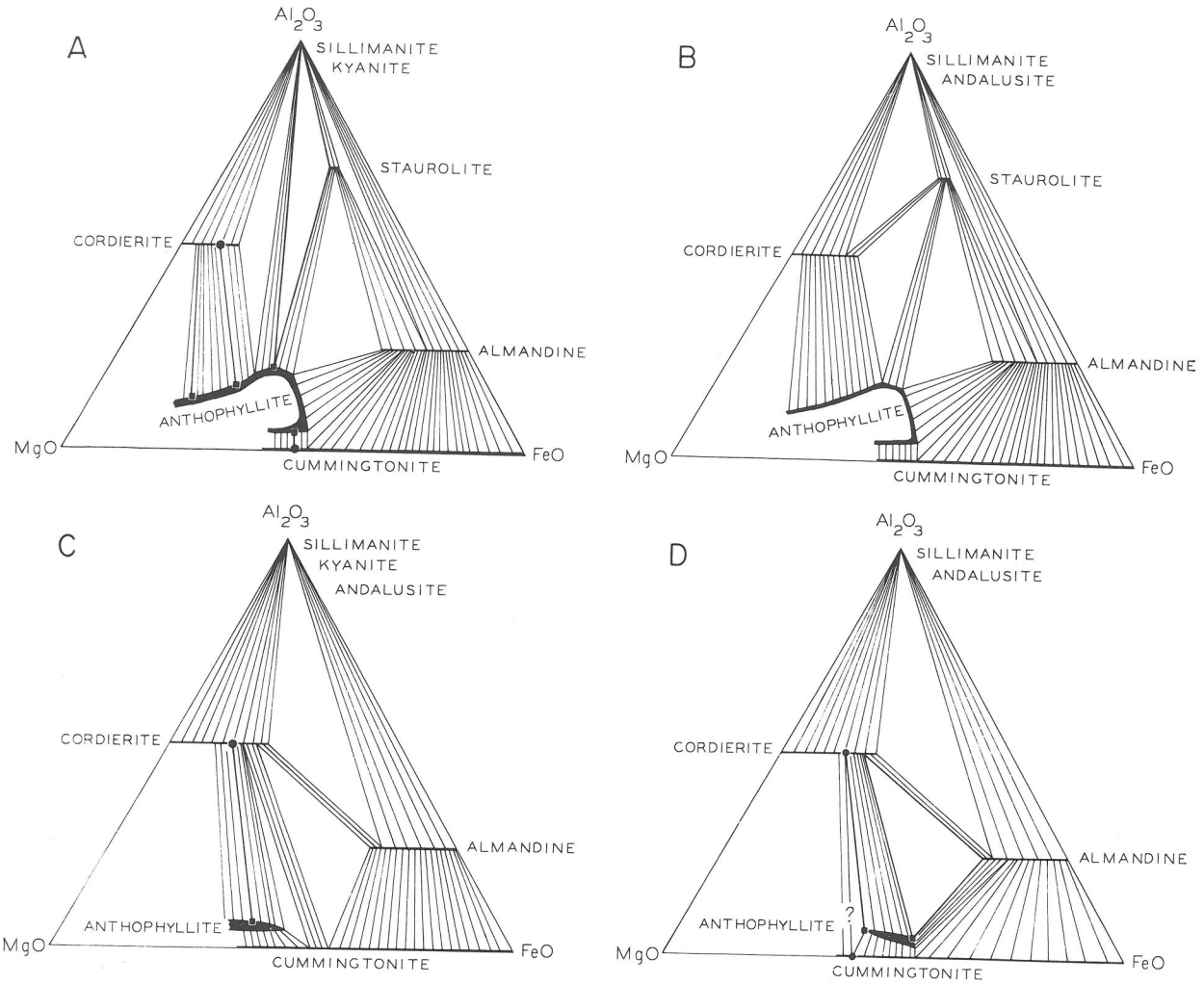

FIG. 13. Several mineral facies of quartz-bearing rocks in the triangle Al_2O_3, MgO, FeO. Anthophyllite analyses plotted on basis of $(Al_2O_3 - CaO - Na_2O)$, MgO, (FeO + MnO).

A. Richmond, New Hampshire (this paper); also Orofino, Idaho (Hietanen, 1959) and Shueretsky District, Kola, U.S.S.R. (Tilley, 1939).

B. Pistil Ogo, Lizard, Cornwall (Tilley, 1937) with andalusite; and Stillwater, Montana (Butler, 1964) with sillimanite. Also Zwart (1962) and Chinner (1966).

C. Trelease Mill and Polkernogo, Lizard, Cornwall (Tilley, 1937) with kyanite and sillimanite, and Träskböle, Orijärvi, Finland (Eskola, 1914) with andalusite and sillimanite.

D. Modified version of C based on limited optical data and partial analysis of cummingtonite coexisting with cordierite at Träskböle.

apparently surrounded by anthophyllite (Eskola, Plate V). Using analyses of coexisting cordierite and anthophyllite of Eskola and expected chemographic relations as a guide, the facies of these two areas would seem to be similar to Figure 13C with a critical assemblage cordierite-anthophyllite-cummingtonite in which cummingtonite is slightly higher in Fe than coexisting anthophyllite. At Trelease Mill coexisting kyanite and sillimanite are characteristic of more aluminous rocks, whereas at Orijärvi the aluminum silicate minerals are andalusite and sillimanite. Staurolite is not present at either locality. Of special note is the low Al_2O_3 content of the analyzed anthophyllite coexisting with cordierite which is in keeping with the expanded compatibilities of cordierite as compared to the "Amphibole Hill" area.

More careful examination of the limited compositional information on cummingtonite and anthophyllite from Trelease Mill and Orijärvi would suggest the relations of Figure 13C are oversimplified. The refractive indices of the cummingtonite from Trelease Mill, $\gamma = 1.665$, and Orijärvi, $\gamma = 1.667$, and a partial analysis of the Orijärvi cummingtonite giving 100 FeO/(FeO + MgO) = 40 all indi-

cate the cummingtonite is more magnesian than the anthophyllites. A second analyzed "dark anthophyllite" is still more Fe rich and apparently coexists with garnet as well as cordierite. These data suggest a more complex topology as shown in Figure 13D. The anthophyllite rim between cummingtonite and cordierite described from both localities could indicate that the growth of anthophyllite is a prograde reaction, but this seems likely only if it is a dehydration reaction involving H_2O-rich cordierite (Schreyer and Yoder, 1964; Robinson and Jaffe, 1969). It is indeed possible that the first appearance of anthophyllite is at the expense of cordierite and cummingtonite that are relatively Fe-rich, the reaction then proceeding to more magnesian compositions. In view of the paucity of analytical data and difficulties in treating hydrous cordierite, the topology of Figure 13C has been chosen for the phase analysis below and cordierite has been assumed to be anhydrous.

Finally in southwestern Montana, Rabbitt (1948) reported the assemblage quartz-anthophyllite-staurolite-cummingtonite. The staurolite-cummingtonite association can be considered an alternative to the garnet-anthophyllite association shown on Figures 13A and 13B.

The facies discussed above are separated by equilibrium reactions. The effect of P and T on these can be evaluated and a simplified P-T grid developed showing relative conditions of formation, as has been done for mica schists by Albee (1965b). Because of extensive solid solution, reactions are hard to evaluate unless assumed fixed compositions are used (Albee, 1965b) as shown in Figure 14 and Table 7. Dashed lines in Figure 14 indicate all observed two phase associations in quartz-bearing rocks. No reports were found of coexisting quartz, aluminum silicate, and cummingtonite; hence, only two out of a theoretically pos-

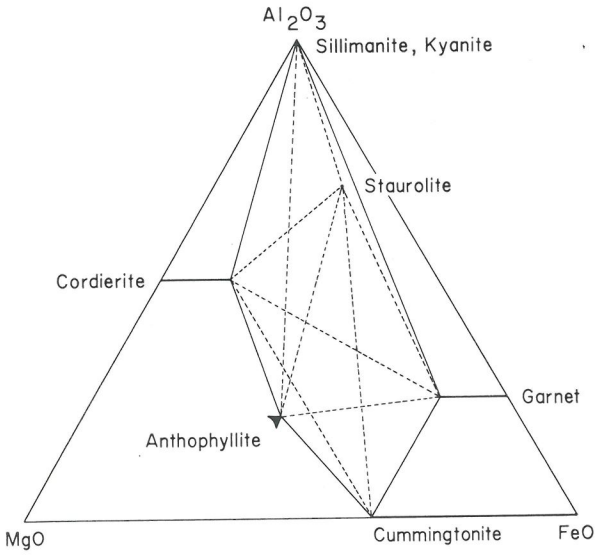

FIG. 14. Fixed compositions and permitted mutual associations of minerals used in calculating P-T grids. Quartz is present as an additional phase in all associations.

TABLE 7. ASSUMED COMPOSITIONS AND MOLAR VOLUMES USED IN CALCULATIONS

Aluminous Anthophyllite	$Mg_{3.0}Fe_{2.5}Al^{VI}_{1.5}Al^{IV}_{1.5}Si_{6.5}O_{22}(OH)_2$	265cc[a]
Cummingtonite	$Mg_{2.5}Fe_{4.5}Si_8O_{22}(OH)_2$	273cc[b]
Cordierite	$Mg_{1.5}Fe_{0.5}Al^{IV}_4Si_5O_{18}$	233cc[c]
Staurolite	$Mg_{0.5}Fe_{1.5}Al^{VI}_9Si_{3.75}O_{22}(OH)^d_2$	223cc[e]
Garnet	$Mg_{0.5}Fe_{2.5}Al^{VI}_2Si_3O_{12}$	115cc[f]
Kyanite	$Al^{VI}_2SiO_5$	44.1cc[g]
Sillimanite	$Al^{VI}Al^{IV}SiO_5$	49.9cc[g]
Quartz	SiO_2	22.7cc[g]

[a] Calculated from cell volumes of Al anthophyllites of Rabbitt (1948).
[b] Calculated from cell volumes given by Klein (1964, Fig. 6).
[c] Schreyer and Schairer, 1961.
[d] From Richardson, 1967, and Schreyer and Chinner, 1967.
[e] Juurinen, 1956.
[f] Skinner, 1956.
[g] Robie, 1966.

TABLE 8. CALCULATED SLOPES OF EQUILIBRIA IN BARS/°C AT 600°C, 5KBAR HIGH T ASSEMBLAGE IS SHOWN ON THE RIGHT

	$PH_2O = Ps$	"Fissure Equilibrium"
36 Staur+34 Cumm+35 Qz→44 Cord +74 Gar+70 H_2O	23.7	46.3
444 Anth+100 Staur+1273 Qz→558 Cord+218 Cumm+326 H_2O	10.9	13.4
32 Anth+218 Kyan+4H_2O→52 Cord +36 Staur+31 Qz	4.0	3.9
52 Cord+36 Staur+31 Qz→32 Anth +218 Sill+4H_2O	−4.9	−4.7
386 Cumm+212 Staur→264 Anth+558 Gar+493 Qz+334 H_2O	$\sim\infty$	−41.8
350 Staur+766.5 Qz→28 Anth+182 Gar+1351 Kyan+322 H_2O	−396	−33.2
350 Staur+766.5 Qz→28 Anth+182 Gar+1351 Sill+322 H_2O	38.7	115.6
14 Anth+38 Kyan+23 Qz→25 Cord +9 Gar+14 H_2O	11.0	15.4
14 Anth+38 Sill+23 Qz→25 Cord +9 Gar+14 H_2O	10.5	13.3
54 Anth+25 Gar+143 Qz→53 Cord +38 Cumm+16 H_2O	0.84	0.93
28 Staur+65 Qz→4 Cord+16 Gar+102 Kyan+28 H_2O	97.0	−63.4
28 Staur+65 Qz→4 Cord+16 Gar+102 Sill+28 H_2O	34.2	78.6
102 Anth+76 Staur+334 Qz→193 Cord +109 Gar+178 H_2O	15.2	21.2

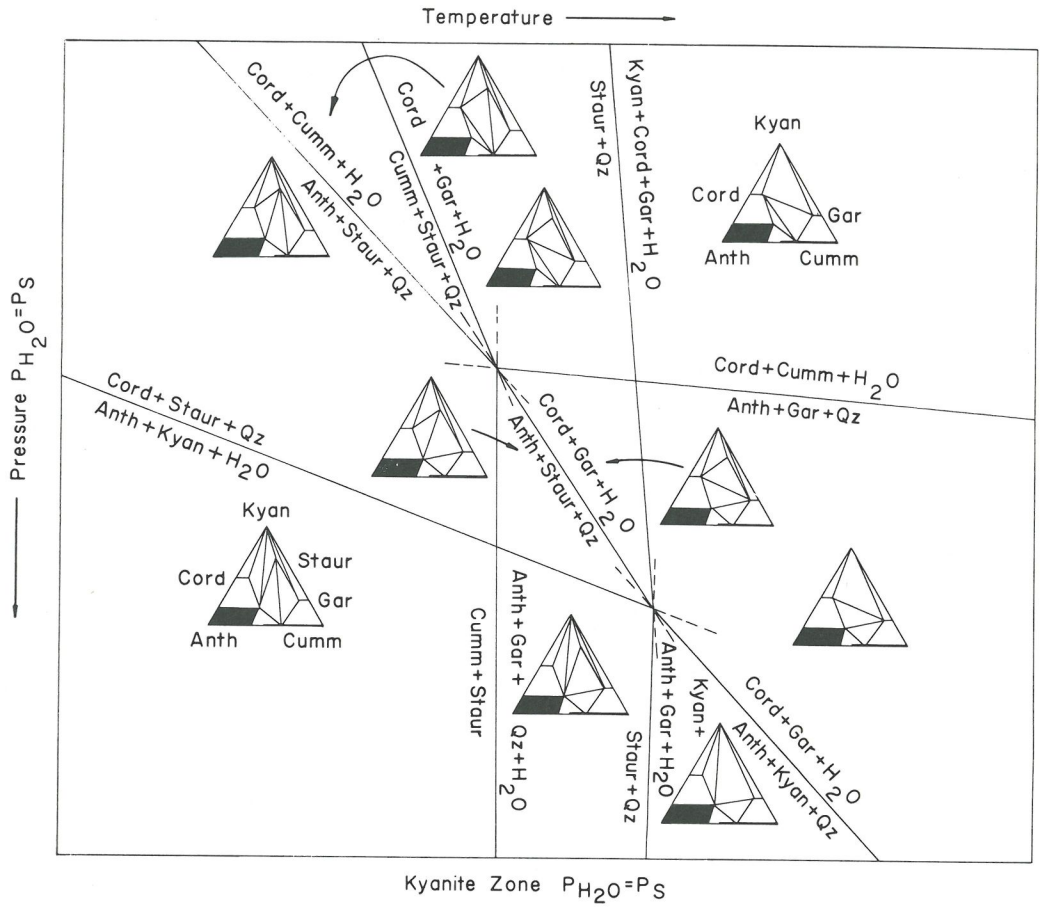

FIG. 15. Calculated *P-T* grid for the kyanite zone showing ten facies types. *P-T* slopes shown are based on relative scale such that 1 kbar on the pressure scale is equivalent to 100°C on the temperature scale.

sible six invariant points appear to be stable. Equilibria involving lower grade chlorites and other more hydrous minerals, or higher grade orthopyroxenes and iron olivines are omitted.

For an assumed P and T of 5 kbar and 600°C, ΔS is taken as 544 dJ/deg[a] per mole of dehydration of H_2O plus 80 dJ/deg[1] per atom of Al changing from VI to IV coordination; ΔV is based on the difference in molar volume of the solids (Table 7) plus a volume of 22 cc per mole[a] of H_2O dehydrated. Albee has considered two special cases from a possible continuum of relations between P_{H_2O} and P solid. Case I, $P_{H_2O} = P_{solid}$. Case II $P_{H_2O} < P_{solid}$ where P_{H_2O} is that to be expected in a water-filled fissure extending to the surface ("fissure equilibrium," Thompson, 1955). For 5 kbar, 600°C.

Case I:
$$\frac{dP}{dT} = \frac{\Delta S}{\Delta V} = \frac{544\text{dJ/deg} + \dfrac{\Delta S(\text{Al}^{\text{VI}} \rightarrow \text{Al}^{\text{IV}})}{n\text{H}_2\text{O}}}{\dfrac{\Delta V \text{ solid}}{n\text{H}_2\text{O}} + 22}$$

[a] Detailed references for derivation of these values are given by Albee 1965b, p. 516.

Case II:
$$\frac{dP}{dT} = \frac{\Delta S}{\Delta V} = \frac{544\text{dJ/deg} + \dfrac{\Delta S(\text{Al}^{\text{VI}} \rightarrow \text{Al}^{\text{IV}})}{n\text{H}_2\text{O}}}{\dfrac{\Delta V \text{ solid}}{n\text{H}_2\text{O}} + 6.7}$$

For reactions involving aluminum silicate, ΔS and ΔV, hence dP/dT, depend on whether the aluminum silicate is kyanite, sillimanite, or andalusite (Table 8). Separate grids have been calculated for both kyanite and sillimanite for Case I (Figs. 15, 16A) and Case II (Figs. 16C, D). Another grid is shown (Fig. 16B) with the kyanite-sillimanite boundary passing through the center. Since the facies under discussion apparently occur within the stability fields of all three aluminum-silicate polymorphs, and since the shape and positions of all of the other equilibria are influenced by variation in P_{H_2O}, various topologic relations between the equilibria and the polymorphic boundaries are to be expected. The equilibria involving anhydrous cordierite (Fig. 15) all have positive slopes with cordierite on the high T, low P side. The effect of hydrous cordierite on these equilibria would be to lower the slopes or even cause them to become negative as in the cases of the experimen-

tally studied reactions Fe-cordierite→almandine + sillimanite + quartz + H_2O (?) (Richardson, 1968) and Mg-cordierite→enstatite + sillimanite + quartz + H_2O (Schreyer and Seifert, 1969, p. 377–379). Such a negative slope for a reaction producing anthophyllite from cordierite and cummingtonite would perhaps partially explain the textural relations observed at Trelease Mill and Orijärvi.

The *P-T* grid has two invariant points, one not involving aluminum silicate, the other not involving cummingtonite. From these points radiate nine univariant reactions separating ten topological facies types. The three anthophyllite-aluminum silicate facies occur at relatively low temperature and high pressure. The five cordierite-staurolite facies occur at relatively intermediate temperature and low pressure. The cordierite-cummingtonite facies appear at relatively low pressure and high temperature.

Summary

1. Composition relations of three amphibole groups occurring within a region of restricted *P-T* conditions indicate that the cummingtonites are compositionally simple, but that the anthophyllites contain nearly the same variety of Na/Al and Al/Al substitution as do the hornblendes.

2. The compositional field of anthophyllite is irregular and no valid distinction between anthophyllite and gedrite can be made except on the basis of X-ray single-crystal

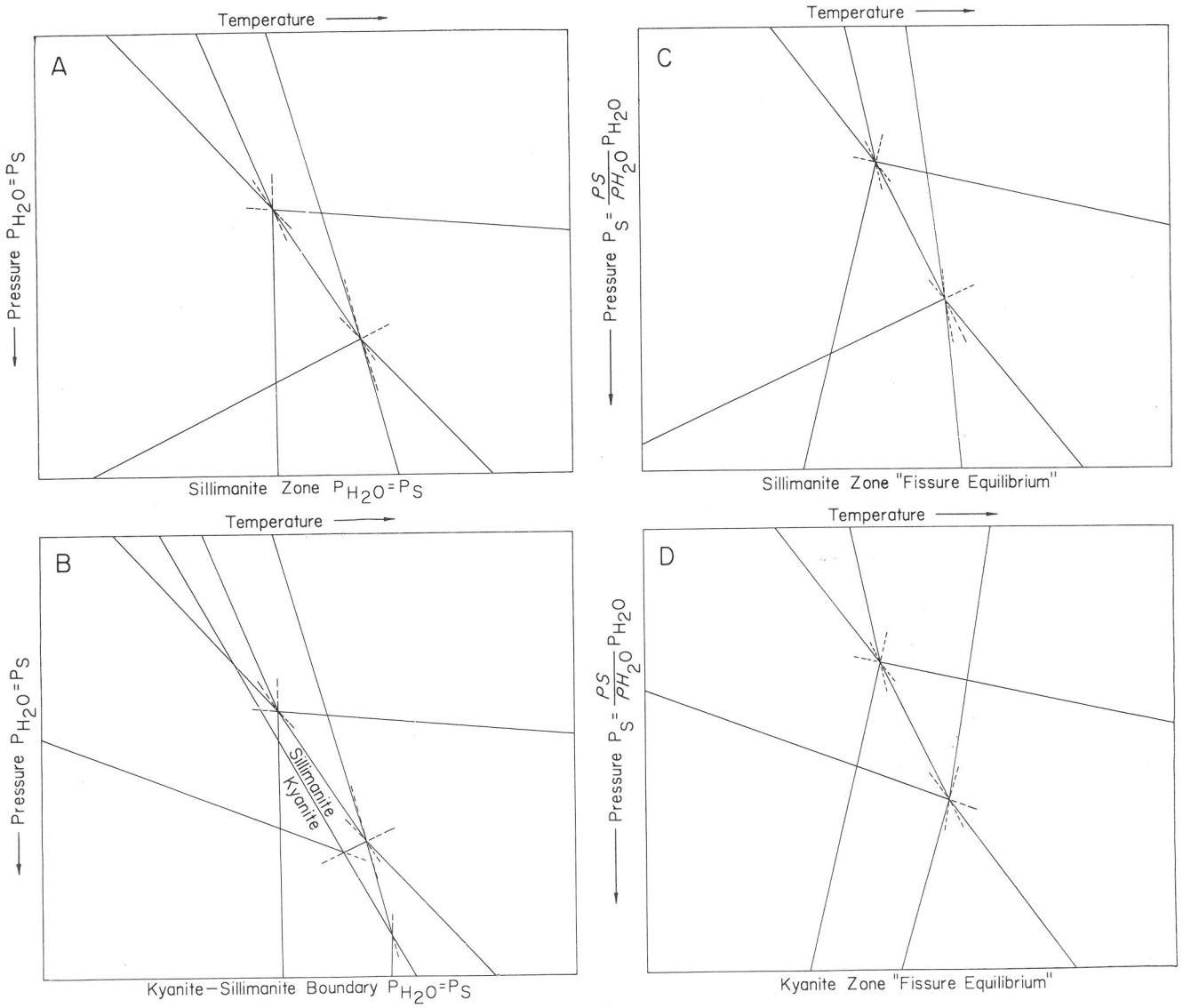

FIG. 16. Calculated *P-T* grids for four assumed conditions. *P-T* slopes shown are based on relative scales such that 1 kbar on the pressure scale is equivalent to 100°C on the temperature scale.

photographs which demonstrate very fine to submicroscopic exsolution of two orthorhombic amphiboles that differ in their b dimensions.

3. For a very limited bulk composition, a stable three amphibole field can be demonstrated: hornblende (with cummingtonite lamellae), cummingtonite (with hornblende lamellae), and anthophyllite (with submicroscopic gedrite lamellae).

4. Bulk compositions rich in Al_2O_3, MgO, and FeO containing anthophyllites, cummingtonites, and other minerals are rare but sufficiently abundant on a world-wide basis to allow recognition of a series of different metamorphic facies. The relative P-T conditions of formation of these facies can be related on a theoretically derived grid.

Acknowledgments

This paper was first prepared for presentation at a seminar on amphiboles held at the University of Massachusetts in March 1968 and has benefited from the comments of many participants. The authors particularly acknowledge the contributions of Cornelis Klein, Jr., Harvard University, who made all of the electron-probe analyses reported here (Klein, 1968), and Malcolm Ross, U. S. Geological Survey, who provided all of the single-crystal X-ray data. Klein and Ross have also provided critical advice and encouragement throughout the work. W. P. Freeborn assisted with the thermodynamic and ratio calculations. Specimen collection, mineral separation, and wet analyses were supported by a University of Massachusetts Faculty Research Grant to Robinson, and National Science Foundation Research Grant GA-467 to Jaffe and Robinson. The authors were assisted at various times in this work by Sergio Deganello who purified most of the amphiboles, David J. Hall, Sherman Clebnik, Peter Gleba, and Walter Trzcienski. Specific acknowledgments for support and assistance in field mapping are given in Robinson (1967) and Thompson, Robinson, Clifford and Trask (1968). Most recently field work was supported by NSF Grant GA-390 to Robinson. The authors wish to thank W. G. Ernst, Malcolm Ross, and B. A. Morgan for their critical review of the manuscript.

References

Albee, A. L. (1965a) Phase equilibria in three assemblages of kyanite-zone pelitic schists, Lincoln Mountain quadrangle, central Vermont. *J. Petrology,* **6,** 246–301.

——— (1965b) A petrogenetic grid for the Fe-Mg silicates in pelitic schists. *Amer. J. Sci.,* **263,** 512–536.

Binn, R. A. (1965) The mineralogy of metamorphosed basic rocks from the Willyama Complex, Broken Hill District, New South Wales, Part I. Hornblendes. *Mineral. Mag.,* **35,** 306–326.

Butler, J. R. (1964) Contact metamorphism along the base of the Stillwater Complex, Montana (abstr.). *Geol. Soc. Amer. Spec. Pap.,* **82,** 24.

Chayes, F. (1944) Petrographic analysis by fragment counting. *Econ. Geol.,* **39,** 489–504.

Chinner, G. A. (1966) The distribution of pressure and temperature during Dalradian metamorphism. *Geol. Soc. London Quart. J.,* **112,** 159–186.

Colville, P. A., W. G. Ernst, and M. C. Gilbert (1966) Relations between cell parameters and chemical compositions of monoclinic amphiboles. *Amer. Mineral.,* **51,** 1727–1754.

Dodge, F. C. W., J. J. Papike, and R. E. Mays (1968) Hornblendes from granitic rocks of the Central Sierra Nevada batholith, California. *J. Petrology,* **9,** 378–410.

Emerson, B. K. (1895) Mineralogical lexicon of Franklin, Hampshire and Hampden Counties, Massachusetts. *U.S. Geol. Surv. Bull.,* **126.**

Ernst, W. G. (1968) *Amphiboles.* Springer-Verlag, New York.

Eskola, P. (1914) On the petrology of the Orijärvi region in southwestern Finland. *Bull. Comm. Geol. Finlande,* **40.**

Green, J. C. (1960) *Geology of the Errol Quadrangle, New Hampshire-Maine.* Ph.D. Thesis, Harvard Univ.

Hallimond, A. F. (1943) On the graphical representation of the calciferous amphiboles. *Amer. Mineral.,* **28,** 65–89.

Hietanen, A. (1959) Kyanite-garnet gedritite near Orofino, Idaho. *Amer. Mineral.,* **44,** 539–564.

Jaffe, H. W., Peter Robinson, and Cornelis Klein, Jr. (1968) Exsolution lamellae and optic orientation of clinoamphiboles. *Science,* **160,** 776–778.

Juurinen, A. (1956) Composition and properties of staurolite. *Ann. Acad. Sci., Fennicae, ser. A, III (Geol. Congr.),* No. 47.

Klein, Cornelis, Jr. (1964) Cummingtonite-grunerite series: a chemical, optical, and X-ray study. *Amer. Mineral.,* **49,** 963–982.

——— (1968) Coexisting amphiboles. *J. Petrology,* **9,** 281–330.

Kretz, R. (1963) Distribution of magnesium and iron between orthopyroxene and calcic pyroxene in natural mineral assemblages. *J. Geol.,* **71,** 773.

Leake, B. E. (1965) The relationship between composition of calciferous amphibole and grade of metamorphism. *In* Pitcher, W. S. and G. W. Flinn (Eds.) *Controls of Metamorphism.* Oliver and Boyd, Edinburgh and London.

——— (1968) A catalog of analyzed calciferous and subcalciferous amphiboles together with their nomenclature and associated minerals. *Geol. Soc. Amer. Spec. Pap.,* **98.**

Rabbitt, J. C. (1948) A new study of the anthophyllite series. *Amer. Mineral.,* **33,** 263–323.

Richardson, S. W. (1967) The stability of Fe-staurolite + quartz. *Carnegie Inst. Wash. Year Book,* **66,** 398–402.

——— (1968) Staurolite stability in a part of the system Fe-Al-Si-O-H. *J. Petrology,* **9,** 467–488.

Robie, R. A. (1966) Thermodynamic properties of minerals *in* Clark, S. P., Jr., Handbook of Physical Constants, *Geol. Soc. Amer. Mem.,* **97,** 437–458.

Robinson, Peter (1963) *Gneiss Domes of the Orange Area, Mass. and N. H.* Ph.D. thesis, Harvard University.

——— (1966) Aluminum silicate polymorphs and Paleozoic erosion rates in central Massachusetts (abstr.). *Trans. Amer. Geophys. Union,* **47,** 424.

——— (1967) Gneiss domes and recumbent folds of the Orange area, west central Massachusetts. *Guideb. New England Intercollegiate Geol. Conf.,* Amherst, Mass. 17–47.

——— and H. W. Jaffe (1969) Aluminous enclaves in gedrite-cordierite gneiss from southwestern New Hampshire. *Amer. J. Sci.,* **267,** 389–421.

———, ———, Cornelis Klein, Jr., and Malcolm Ross (1969) Equilibrium coexistence of three amphiboles. *Contrib. Mineral. Petrology* (in press).

Ross, Malcolm, J. J. Papike, and K. W. Shaw (1969) Exsolution in amphiboles. *Mineral. Soc. Amer. Spec. Paper.* **2,** 275–299.

———, ———, and P. W. Weiblen (1968) Exsolution in clinoamphiboles. *Science,* **159,** 1099.

Schreyer, W., and G. A. Chinner (1966) Staurolite-quartzite bands in kyanite quartzite at Big Rock, Rio Arriba County, New Mexico. *Contrib. Mineral. Petrology,* **12,** 223–244.

———, and J. F. Schairer (1961) Compositions and structural states of anhydrous Mg-cordierites: a reinvestigation of the

central part of the system $MgO-Al_2O_3-SiO_2$. *J. Petrology*, **2,** 324.

———, AND F. SEIFERT (1969) Compatibility relations of the aluminum silicates in the systems $MgO-Al_2O_3-SiO_2-H_2O$ and $K_2O-MgO-Al_2O_3-SiO_2-H_2O$. *Amer. J. Sci.*, **267,** 371–388.

———, AND H. S. YODER (1964) The system Mg-cordierite-H_2O and related rocks. *Neues Jahrb. Mineral.*, **101,** 271–342.

SHIDO, FUMIKO (1958) Plutonic and metamorphic rocks of the Nakoso and Irituno districts in the Central Abukuma plateau. *J. Fac. Sci., Univ. Tokyo* **11,** 131–217.

SKINNER, B. J. (1956) Physical properties of end members of the garnet group. *Amer. Mineral.*, **41,** 428.

THOMPSON, J. B., JR. (1947) Role of aluminum in the rock-forming silicates. *Geol. Soc. Amer. Bull.*, **58,** 1232.

——— (1955) Thermodynamic basis for the metamorphic facies concept. *Amer. J. Sci,* **253,** 65–103.

——— (1957) The graphical analysis of mineral assemblages in pelitic schists. *Amer. Mineral.*, **42,** 842–858.

———, PETER ROBINSON, T. N. CLIFFORD, AND N. J. TRASK, JR. (1968) Nappes and gneiss domes in west-central New England *in* Zen, E-an, and W. S. White (Eds.), *Studies of Appalachian Geology—Northern and Maritime.* John Wiley & Sons, New York, 203–218.

TILLEY, C. E. (1937) Anthophyllite-cordierite granulites of the Lizard. *Geol. Mag.*, **74,** 300–309.

——— (1939) The kyanite-gedrite paragenesis. *Geol. Mag.*, **76,** 326–330.

WINCHELL, A. N. (1945) Variations in composition and properties of the calciferous amphiboles. *Amer. Mineral.*, **30,** 27–51.

ZWART, H. J. (1962) On the determination of polymetamorphic mineral associations and its application to the Bosost area (Central Pyrenees). *Geol. Rundsch.*, **52,** 38–65.